Earth Planet. Sci. Lett. 643 (2024) 118895

Contents lists available at ScienceDirect

Earth and Planetary Science Letters

journal homepage: www.elsevier.com/locate/epsl

Mantle deformation in the highly oblique indo-burma subduction system inferred from shear wave splitting measurements

Md Mohimanul Islam [a,*], Shengji Wei [b], Patricia Persaud [c], Michael S. Steckler [d], Frederik Tilmann [e,i], James Ni [f], James Gaherty [g], Kyaw Moe Oo [h], Oo Than [h], Yin Myo Min Htwe [h], Eric Sandvol [a]

[a] Department of Geological Sciences, University of Missouri, Columbia, MO, USA
[b] Earth Observatory of Singapore/Asian School of the Environment, Nanyang Technological University, Singapore
[c] Department of Geosciences, University of Arizona, Tucson, AZ, USA
[d] Lamont Doherty Earth Observatory, Columbia University, Palisades, NY, USA
[e] GFZ German Research Centre for Geosciences, Telegrafenberg, Germany
[f] Department of Physics, New Mexico State University, Las Cruces, NM, USA
[g] School of Earth and Sustainability, Northern Arizona University, Flagstaff, AZ, USA
[h] Department of Meteorology and Hydrology, Naypyitaw, Myanmar
[i] Institute for Geological Sciences, Freie Universität Berlin, Germany

ARTICLE INFO

Edited by: Dr H Thybo

Keywords:
Seismic anisotropy
Shear wave splitting
Mantle deformational fabric
Trench parallel mantle flow
Oblique subduction
Hainan Plume

ABSTRACT

We utilized shear wave splitting analysis of teleseismic SKS, SKKS, and PKS phases to infer upper mantle deformational fabrics across a substantial area of Southeast Asia, where splitting measurements were previously limited. We used newly available permanent and temporary broadband seismic networks deployed across the Indo-Burma subduction zone and the eastern Indochina peninsula. The resulting 492 well-constrained splitting and 654 null measurements from 185 stations reveal clear large-scale patterns in the mantle deformational fabrics in response to the highly oblique active subduction and a large transform plate boundary. We identified two distinct domains of mantle deformation fabrics in the western Burma microplate and the eastern Indochina peninsula. In the former, trench parallel N-S fast polarization directions with an average lag time (δt) of 1.9 s are observed beneath the Indo-Burman Ranges. We suggest the observed splitting is partly due to anisotropy in the sub-slab region and relates to shear induced by the north moving Indian plate. The lithospheric fabric within the Indo-Burman Ranges and underlying subducting slab fabric contribute to produce the observed average δt of 1.9 s. The δt value decreases to an average of 1.0 s towards the back-arc until we reach the dextral Sagaing fault. In the second domain, starting approximately 100 km east of the Sagaing fault, we observe a consistent E-W fast direction with an average δt of 1.10 s in the eastern Shan-Thai and Indochina blocks. We interpret the E-W fabric as due to the deformation associated with the westward spreading of the Hainan mantle plume, possibly driven by overriding plate motion. Low velocities in the shallow mantle and late Cenozoic intraplate volcanism in this region support the plume-driven asthenospheric flow model in the Indochina peninsula. The sudden transition of the fast polarization direction from N-S to E-W along the eastern edge of the Burma microplate indicates the Sagaing fault acts as a mantle flow boundary between the subduction dominated trench parallel flow to the west and plume induced asthenospheric flow to the east. We also observed no net splitting beneath the Bengal basin which is most likely due to the presence of frozen vertical fabric resulting from the Kerguelen plume activity during Early Cretaceous.

1. Introduction

Southeast Asia offers an excellent natural laboratory to study the nature of upper mantle deformation and flow related to the largest continental collision on earth (e.g. Tibet) as well as the mantle deformation related to an active plume (e.g. Hainan Island). Active

* Corresponding author.
E-mail address: mibhk@umsystem.edu (M.M. Islam).

https://doi.org/10.1016/j.epsl.2024.118895
Received 28 December 2023; Received in revised form 7 July 2024; Accepted 12 July 2024

convergence of the Indo-Australia plate with the Eurasia plate has shaped the Cenozoic tectonic evolution of southeast Asia (Keep and Schellart, 2012; Zahirovic et al., 2014). The northward motion of the Indian plate and its subsequent collision with Eurasia created a broad and diffuse deformational zone with wide variation in crustal and lithospheric thickness (Le Pichon et al., 1992; Molnar and Tapponnier, 1975; Replumaz and Tapponnier, 2003; Tapponnier et al., 1986). The collisional front takes a sharp N-S bend along the eastern Himalayan syntaxis (EHS) and transitions into an extremely oblique subduction where the Indian plate is subducting beneath the Burma microplate, commonly known as the Indo-Burma subduction zone (IBSZ; Fig. 1).

Observations of seismic anisotropy can help to infer both present-day deformation in the upper mantle as well as preserved deformational fabrics frozen into the mantle lithosphere (Long and Becker, 2010). Within the dislocation creep domain in the upper mantle, simple shear leads to the development of lattice-preferred orientation (LPO) of olivine, resulting in a directional dependence of seismic velocity (Christensen, 1984; Karato et al., 2008; Savage, 1999; Silver and Chan, 1991) that can be measured via shear wave splitting (SWS). It is well known that the polarization direction of the fast shear wave [φ] and the time delay between the fast and slow shear waves [δt] are the two parameters that can be used to characterize SWS. Due to the lack of vertical resolution, SWS measurements in a subduction system reflect an integrated effect of anisotropy in the sub-slab mantle, slab, and mantle wedge, which in other contexts can be difficult to isolate (Long and Silver, 2009; Long and Wirth, 2013).

Previous investigations of SWS (L. Chang et al., 2015; León Soto et al., 2012; McNamara et al., 1994; Sol et al., 2007; J. Wang and Zhao, 2008) and crustal deformation from GPS (Gan et al., 2007; Liang et al., 2013; M. Wang and Shen, 2020) in the eastern India-Eurasian collisional zone (Fig. 2) strongly suggests a vertically coherent upper mantle and crustal deformation with a clockwise rotation around the EHS. This

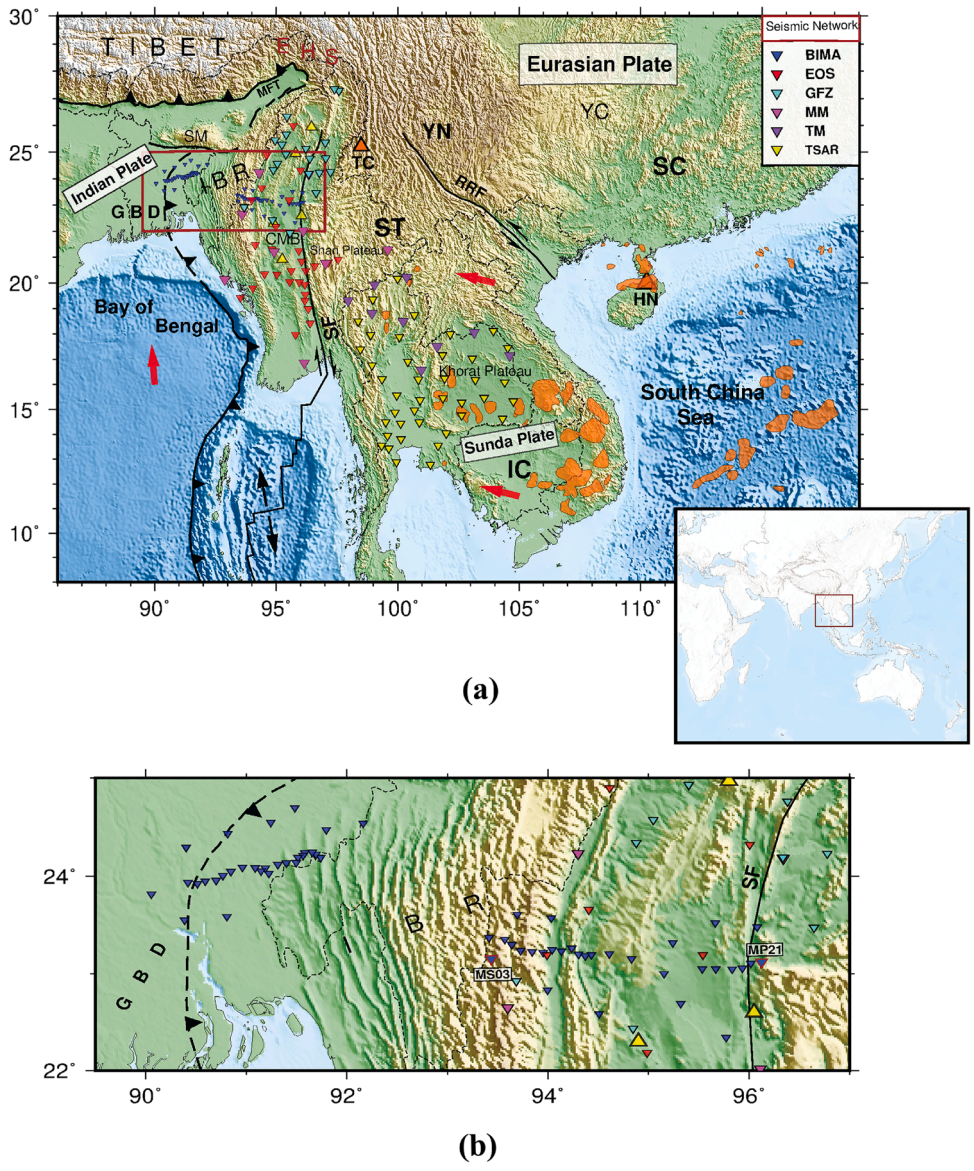

Fig. 1. (a) Distribution of seismic networks and simplified tectonic map of the study area; Red arrows show the absolute plate motion direction according to the hotspot HS3-NUVEL 1A model (Gripp and Gordon, 2002). The orange upright triangles show Tengchong and Hainan volcanic centers. Yellow upright triangles show Late Cenozoic volcanic centers in Myanmar (from Lee et al., 2016; Searle et al., 2007). The orange polygons show the distribution of Late Cenozoic (< 16 Ma) intraplate volcanism from Yan et al., 2018. CMB – Central Myanmar Basin; EHS – Eastern Himalayan Syntaxis; GBD – Ganges Brahmaputra Delta; HN – Hainan; IBR – Indo-Burman Range; IC – Indochina Block; MFT – Main Frontal Thrust; RRF – Red River Fault; SC – South China; SF – Sagaing Fault; SM – Shillong Massif; ST – Shan-Thai Block; TC- Tengchong volcano; YC- Yangtze Craton; YN – Yunnan. (b) Zoom in view of the Ino-Burman subduction system showing the individual station of BIMA seismic network.

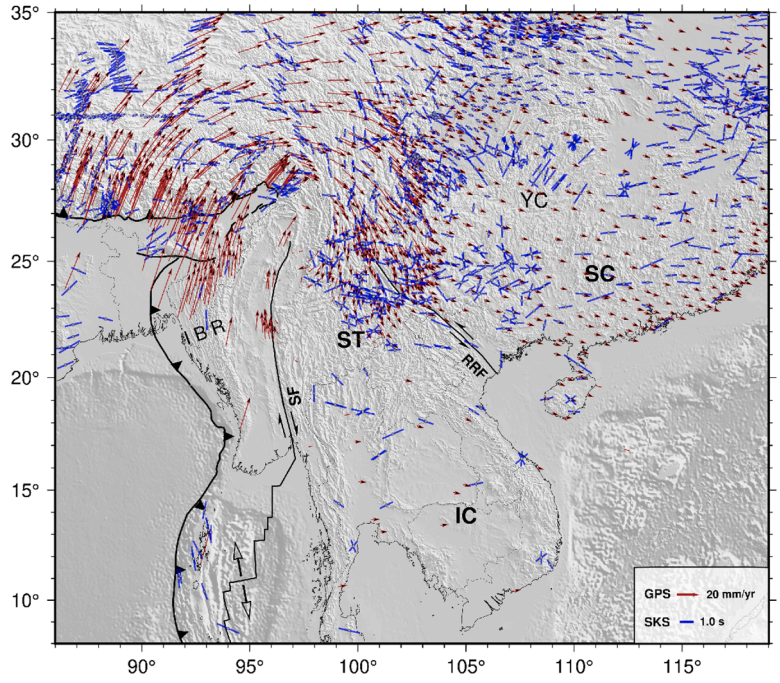

Fig. 2. Previous station average SKS measurements and GPS velocity vectors relative to stable Eurasia. GPS velocity vectors are sourced from (Devachandra et al., 2014; Gupta et al., 2015; Kreemer et al., 2014; Marechal et al., 2016; Vernant et al., 2014; M. Wang and Shen, 2020). Previous SKS results are taken from the SWS database (from Barruol et al., 2009). Abbreviations are the same as in Fig. 1.

clockwise rotational pattern disappears in the southern Yunnan Province near 27°N where the fast direction changes from N-S to E-W (Z. Huang et al., 2007; Lev et al., 2006). The question remains of what drives the mantle flow in the IBSZ and the entire Indochina peninsula. In the IBSZ margin, Russo (2012) first observed a trench parallel fast direction using source-side shear wave splitting measurements and proposed a regional mantle flow model influenced by slab segmentations. Many of the splitting delay times exceed 3.0 s, which is rarely observed elsewhere, suggesting possible receiver side contamination. Later, Liu et al. (2019) proposed whole a India slab rollback model where both the northward and eastward India-Eurasia convergent margins are rolling back along with a large-scale toroidal flow resulting from a slab gap near the EHS; however, the suggested slab gap is not visible in regional travel-time tomographic models (Dubey et al., 2022; Shi et al., 2020) and the westward toroidal flow is not supported by the current geodynamic model where several lines of evidence suggest the eastward asthenospheric flow dominating in southern Tibet. (Agius and Lebedev, 2013, 2017; Jolivet et al., 2018; Ye et al., 2016; Y. Yu et al., 2021). Several recent studies (Fan et al., 2021; Kong et al., 2018; Y. Yu et al., 2018) proposed a westward slab roll-back model that drives the mantle deformation of the entire Burma block and eastern Indochina. Such large-scale roll-back and associated corner flow do not seem to correlate with the absence of back-arc extension and extensive volcanism. We endeavor to determine whether the IBSZ controls mantle flow beneath the western Burma block and eastern stable Indochina.

One key drawback of the previous studies is the lack of SWS spatial coverage across critical tectonic units, especially along the Sagaing fault and eastern Indochina peninsula. Our study covers the entire Indo-Burma subduction regime encompassing the western deformation front to the eastern Indochina peninsula. We have used SWS analysis of the core refracted S waves (SKS, SKKS, PKS, collectively known as XKS) to map the spatial distribution of seismic anisotropy. One contribution of this study is to fill a large gap in shear wave splitting measurements across a significant part of southeast Asia. Taking advantage of the dense network coverage, this study aims to better understand the mantle flow dynamics of this complex system by addressing several key questions including the nature of the N-S to E-W transition of fast direction in the Indochina peninsula, the role of the northward movement of the Indian plate and lithospheric contribution to the overall anisotropy. Another contribution of this study is to provide a framework that explains abrupt changes in shear wave splitting measurements south of the EHS, across the Sagaing Fault, and within the IBSZ.

2. Background

The present N25°E motion of the Indian plate relative to Eurasia (MORVEL56-NNR model, Argus et al., 2011) has a convergent component of 12–24 mmy^{-1} with a dextral component of ~40 mmy^{-1} relative to the Burma platelet (Mallick et al., 2019; Oryan et al., 2023; Steckler et al., 2016). The highly oblique convergence of India along the IBSZ results in strain partitioning of which about half is accommodated by the dextral motion of the Sagaing Fault (Fitch, 1972; Khin et al., 2017; Vigny, 2003). This ~1200 km long fault forms the eastern boundary of the Burma microplate and has an estimated displacement of 400 to 1000 km since the Miocene (Mitchell, 1993; Morley, 2017; Morley and Arboit, 2019; Y. Wang et al., 2014). The oblique convergence also facilitates the northward movement of the overriding Burma microplate relative to the adjacent Sunda plate (Bertrand and Rangin, 2003; Maurin and Rangin, 2009; Morley, 2002). Another unique feature of this subaerial subduction system is its very limited magmatic arc, despite experiencing a substantial sediment influx from the world's largest delta: the Ganges-Brahmaputra Delta (GBD). The ongoing subduction since the Oligocene results in thrusting and crustal shortening of the upper plate (Maurin and Rangin, 2009; Najman et al., 2020), forming the Indo-Burman range (IBR).

Unlike the southern Andaman-Sumatra-Java segments where the Wadati-Benioff zone (WBZ) extends down to ~670 km (Kayal, 2008), the slab earthquakes of the IBSZ have a maximum depth of ~180 km (Dasgupta et al., 2003; Hurukawa et al., 2012; Ni et al., 1989; Rao and Kalpna, 2005; Satyabala, 2003; Stork et al., 2008). Both global and regional traveltime tomographic models have imaged an east-dipping high-velocity slab-like structure descending 100–200 km below the WBZ seismic zone (J. Huang and Zhao, 2006; Koulakov, 2011; Lei and Zhao, 2016; C. Li et al., 2008; Wei et al., 2012); however, there are

significant variations in slab structure and depth extent among these models due to the lack of sufficient station coverage. Recent tomographic models with increased resolution have all found high velocity slab-like structures extending down to the mantle transition zone (MTZ) (Lei and Zhao, 2016; Wei et al., 2012; Yao et al., 2021).

The Sagaing Fault forms the eastern boundary of the stable Sundaland block, an amalgamated continental block formed during the Indonesian Orogeny in the Late Triassic. (Metcalfe, 2011, 2013; Ng et al., 2015; Searle et al., 2012; Sone and Metcalfe, 2008). The segment of the Sundaland block situated southeast of the EHS is recognized as the Indochina peninsula. This tectonic block comprises of the Shan-Thai (ST) and Indochina (IC) blocks and has undergone southeast extrusion and clockwise rotation due to the early India-Eurasia collision(S. Li et al., 2017; Richter and Fuller, 1996; Sato et al., 2007; Takemoto et al., 2009; Z. Yang et al., 2001).

3. Data and methods

3.1. Data

We used data collected from recently deployed temporary and permanent broadband seismic networks deployed in Bangladesh, Myanmar, and Thailand. Among these stations, the Bangladesh-India-Myanmar Array (BIMA) network covers the entire subduction margin, spanning from the western Bengal basin to the eastern central Myanmar basin (CMB) (Fig. 1). Active since early 2018, this profile network consists of 61 stations, deployed in Bangladesh and Myanmar (FDSN XR_2018–2022, Sandvol et al., 2018). The Earth Observatory of Singapore (EOS) network stations are distributed along the Sagaing Fault and the CMB. GFZ stations are mostly located in the northern CMB close to the EHS (FDSN 6C_2018–2022, Tilmann et al., 2021). The Myanmar National Seismic Network (MM), which consists of nine broadband seismic stations, first came online in early 2016 (FDSN MM_2016, Department of Meteorology and Hydrology - National Earthquake Data Center, 2016). TM (FDSN TM_2008_2021) and TSAR networks are distributed in Thailand, covering the southern part of the Shan-Thai block and the Indo-China block. Overall, we have used 185 permanent and temporary stations with a recording period ranging from early 2009 to late 2022. Teleseismic events of magnitude greater than 5.8 have been used to ensure high signal-to-noise (SNR) of the incoming core refracted shear waves. The epicentral distance ranges of 85°−120°, 95°−180°, and 120–180° were selected for analyzing SKS, SKKS, and PKS phases, respectively. The spatial distribution of the teleseismic events is shown in the supplementary material (Fig. S1.2), available in the online version of this article.

3.2. Methods

We have utilized the method of Silver & Chan (1991) to determine the optimal splitting parameters. Using a grid-search approach, the best-fitting splitting parameters are estimated by rotating and time-shifting the seismogram pair that minimizes the energy in the transverse component. An ideal window length has been manually selected, and it typically begins 10–15 s before the incoming XKS waves and includes at least one full cycle of clear arrival. Before measurements, individual seismograms were passed through a bandpass with a corner frequency of 0.03–1.0 Hz to isolate the XKS energy. Uncertainty estimates were carried out following the F-test approach of Silver & Chan (1991) and verified using the bootstrapping method (Sandvol and Hearn, 1994). Each splitting result has undergone quality control by visual inspection to eliminate unreliable results, such as instances where the uncertainties are underestimated. This approach involves the inspection of every splitting waveform, particle motion, transverse energy contour map, and residual tangential energy of the corrected tangential component. Using these criteria, all results are subjectively ranked from Q1 to Q4 (excellent, good, fair, poor) [see supplementary material, Fig. S2.1]. Reliable results all have linear particle motions after applying optimal rotation and time shifts, a clear global minimum energy on the transverse contour map, and small residual energy on the corrected tangential component (Fig. 3). We have also observed null measurements, where a clear S wave arrival is present on the radial component but there is no energy in the transverse components. Station average splitting parameters were calculated taking circular (fast directions) and arithmetic averages (lag times) of Q1 and Q2 quality measurements.

4. Results

A total of 492 well-constrained (Q1 and Q2) splitting parameters and 654 nulls were obtained from 160 different stations. We performed 900 SKS, 212 SKKS, and 34 PKS measurements by analyzing 191 events. In addition, 25 stations were analyzed but did not produce any measurable splitting results, due to either noisy horizontal components with low SNR (especially in Thailand) or limited active service days. These stations are distinct from the null stations which had good SNR waveforms that did not split from a variety of azimuths. The station average splitting measurements are shown in Fig. 4. We primarily observed three distinct types of splitting patterns in our study area. In the western Bengal basin and outer fold belt of the IBR, there is little evidence of splitting. We found 264 well-defined nulls in 28 stations of the BIMA network in Bangladesh. Only a single station (BA17) has a few waveforms with measurable splitting with a maximum lag time of 0.4 s, comparable to typical crustal splitting values (Silver, 1996). Reasonable back-azimuth coverage [supplementary material, Fig. S2.3(a)] ensures that the observed nulls are not resulting from the incoming shear wave being parallel or perpendicular to the fast axis of the anisotropic medium.

In the central IBR and CMB, we observed a consistent trench parallel N-S fast direction with a circular mean of $-3.0 \pm 9.5°$. Along the subduction zone, the fast directions vary slightly from N—NW to N—NE direction as we move from south to north following the curvature of the IBR orogen. The average lag time in the IBR is 1.9 ± 0.4 s, higher than the global average of ~1.0 s for continents (Silver, 1996). Similar trends were also reported in previous studies, although with limited station coverage (Fan et al., 2021; Saikia et al., 2018). The projection of null and splitting measurements at 210 km ray piercing points shows that the higher lag time values of IBR do not overlap with the nulls region in Bengal basin (see supplementary material, Fig. S6.1). The maximum average lag time is observed at station MP01 (2.8 ± 0.5 s), located in the westernmost part of the IBR. The lag time reduces to ~1.0 s in the CMB. The average lag time along the Sagaing fault is higher (1.3 ± 0.4 s) than the surrounding regions, and the fast direction aligns closely with the strike of the fault with a circular mean of $-16.1 \pm 12.7°$.

In Thailand, the fast direction changes from N-S to nearly E-W. All stations in the IC block have a consistent E-W fast direction with an average lag time of ~1.1 s. Previous studies using sparsely distributed stations also reported E-W fast axes (L. Liu et al., 2019; Y. Yu et al., 2018). Interestingly, some stations in the southern ST block in the Shan Plateau have no splitting measurement (i.e., null shear wave splitting).

4.1. Multiple anisotropic layers

In order to look into the potential existence of multiple anisotropic layers, we examined the back-azimuth dependency of the splitting parameters. Periodic variations of apparent splitting parameters relative to the back azimuth are often indicative of multiple anisotropic layers (Silver and Savage, 1994). Complete azimuthal coverage has not been achieved for most of the temporary networks due to the uneven distribution of teleseismic events; however, some stations with reasonably good coverage do not show any periodic variations in splitting parameters with respect to BAZ modulo 90 (supplementary material, Fig. S3.1). The lack of a distinct periodic back-azimuthal dependency of the splitting parameters implies the existence of a single anisotropic

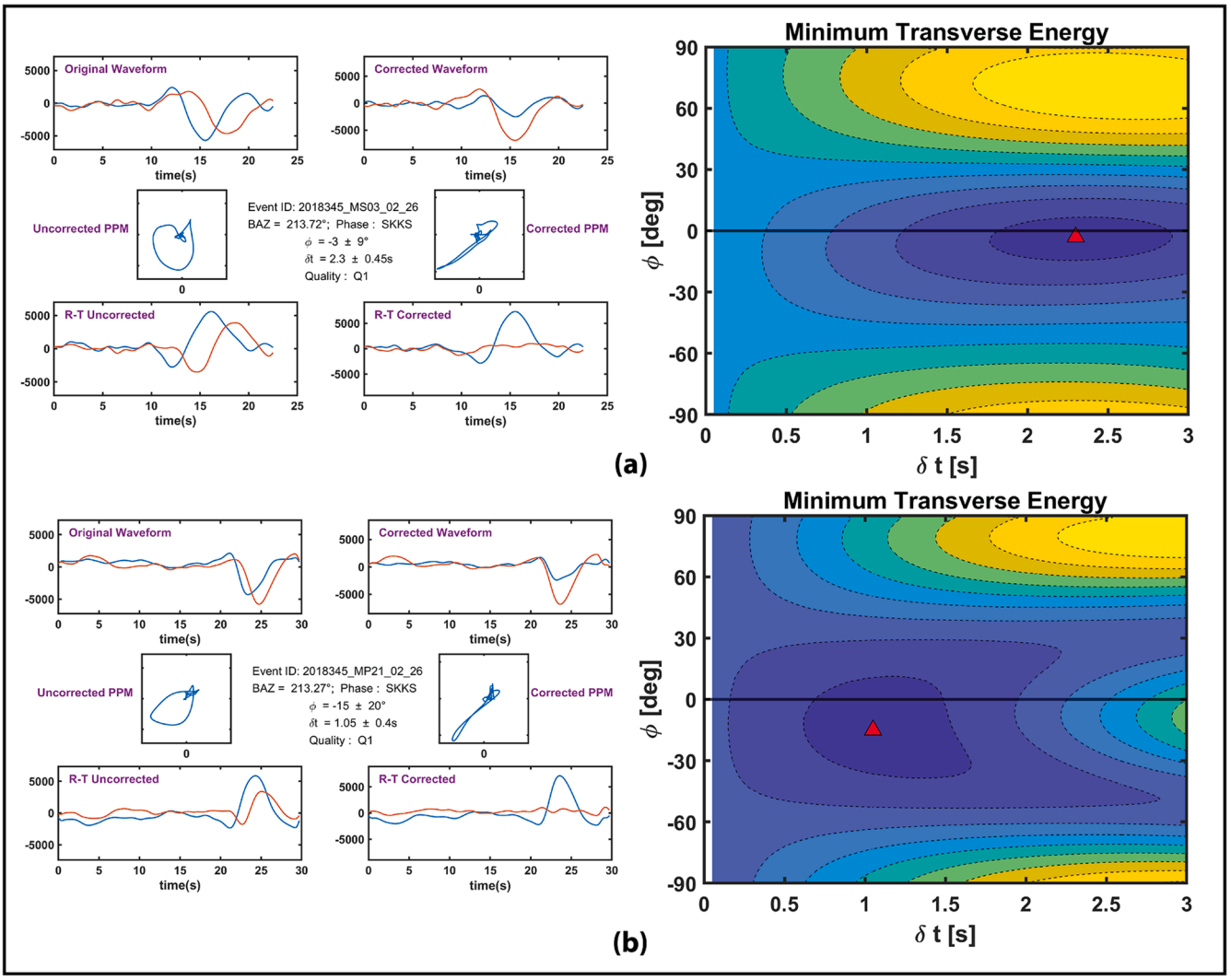

Fig. 3. Example of teleseismic splitting results for the same event recorded at (a) station MS03 with larger δt; (b) station MP21 with average δt. The location of the stations is marked in Fig. 1(b).

layer with a horizontal axis of symmetry. It is important to note that, with the exception of MDY, most stations still have some gaps in the back-azimuth coverage where existence of multiple layers cannot be ruled out.

4.2. Depth of the anisotropic layer

The presence of smooth spatial variations in splitting parameters combined with dense station spacing with decent azimuthal coverage and a single anisotropic layer enables us to apply the spatial coherency technique to estimate the anisotropic depth (K. H. Liu and Gao, 2011). In this method, the spatial variation factor, defined by the weighted sum of the standard deviation of the fast axes (circular) and lag times, is calculated over a depth range of 0 to 400 km in overlapping rectangular blocks (Gao and Liu, 2012). The minimum variation factor corresponds to the optimal depth of the anisotropy (see details in supplementary material, section S4). The curve of variation factors in the eastern Indo-China block has a flat bottom with minimum variation factors obtained for depths of ~200–300 km using a block size of 0.25°, indicating that the primary anisotropy source is below the lithospheric depth (Fig. 5). For IBR and CMB regions, the variation factors did not converge well, probably due to the variation of the splitting parameter with depth, different depths dominating in different sub-regions, or insufficient azimuthal coverage.

5. Discussion

5.1. Trench parallel flow in the IBR

We measured an average lag time of 1.9 s along the IBR margin with trench parallel fast axes, which is larger than that of most other subducting slabs (Long and Silver, 2008). Several studies proposed slab roll-back with toroidal flow model to explain the observed mantle deformation fabric (Fan et al., 2021; L. Liu et al., 2019); however, such roll-back would require well-developed back-arc extension or compression depending on the overriding plate mobility (Nakakuki and Mura, 2013; Schellart and Moresi, 2013). Late Cenozoic surface deformations in the ST and IC blocks are primarily dextral and sinistral motion along major fault systems and widespread sedimentary basin inversion (Searle and Morley, 2011). Earthquakes in Yunnan, Laos, northeast Myanmar, and north Thailand are dominated by strike-slip focal mechanisms, primarily following a NE-SW to ENE-WSE trend (Morley, 2007; Socquet and Pubellier, 2005). Additionally, we observe only a low volume of Quaternary volcanism in central Myanmar (Lee et al., 2016; Maury et al., 2004; L. Y. Zhang et al., 2020) whereas slab roll-back usually results in extensive volcanism from asthenospheric upwelling (e.g., MORB-like diabase dykes in the Chinese Altai, J. Wang et al., 2020; alkaline volcanic complex in the Mediterranean, Prelević et al., 2015; mafic intrusions in North Sumatra, X. Yu et al., 2023).

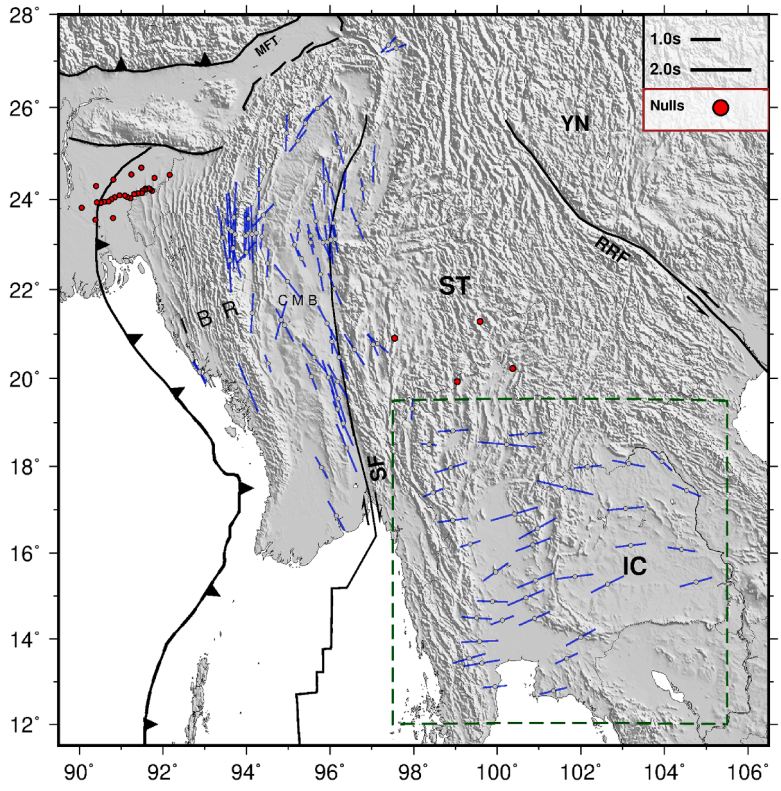

Fig. 4. Station average teleseismic shear wave splitting results of the study area. The green box shows the rectangular area that was considered for calculating the depth of the anisotropy beneath the IC block (Fig. 5).

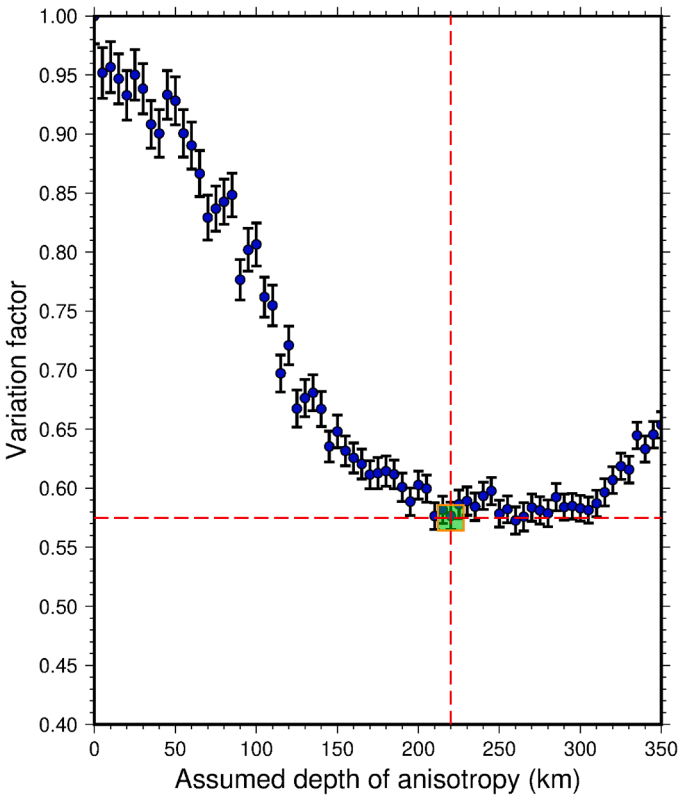

Fig. 5. Spatial variation factors plotted against the depth of anisotropy for the IC block.

In the absence of active slab roll-back, other mechanisms are needed to explain the observed large lag time. Predominant surface deformation in the IBR is ~E-W thrusting with crustal shortening and N-S strike-slip faulting (Betka et al., 2018; Maurin and Rangin, 2009; Najman et al., 2020) due to the oblique convergence since Oligocene (Mon et al., 2020). When we examine the individual splitting measurements, larger δt values correlate with the higher topography (Fig. 6) of the IBR. The strong correlation with the topography as well as lithospheric thickness (Pasyanos et al., 2014) indicate that the IBR anisotropy has a significant lithospheric contribution resulting from E-W tectonic compression with crustal thickening and N-S shearing associated with the ongoing convergence. Additionally, the subducting Indian slab reaches a maximum depth of 60 km beneath the IBR, making a shallow angle subduction before dipping more steeply (Hayes et al., 2018; Hurukawa et al., 2012). Slab anisotropy may have developed from the E-W convergence, thus also contributing to the total IBR anisotropy, which could account for the large (~2 s) lag times.

Absolute plate motion (APM) induced fabric could also contribute to the observed anisotropy in the IBR. The Indian plate close to the IBR is moving N7°W at a rate of ~52 mmyr^{-1}, according to the HS3-NUVEL1A model (Gripp and Gordon, 2002). Several geodynamic models suggest the down dip motion of the Indian slab stopped as it transitioned from oceanic to continental crust (G. Zhang et al., 2021; Zheng et al., 2020). The northward motion of dipping Indian slab along with the Indian plate motion could induce simple shear in the surrounding mantle. Assuming the presence of A-type LPO fabric and alignment of fast directions with the mantle flow direction, this deformation could produce the observed trench parallel flow around the slab. In the mantle wedge, the combination of high-water content and elevated stress conditions may promote the formation of B-type olivine fabric, as suggested by Fan et al., 2024. However, the presence of short-lived, low-volume arc volcanoes is not consistent with pervasive high water content in this mantle wedge (Zhang et al., 2020). Therefore, the fore-arc water enriched zone suitable for B-type development should be limited where water content can

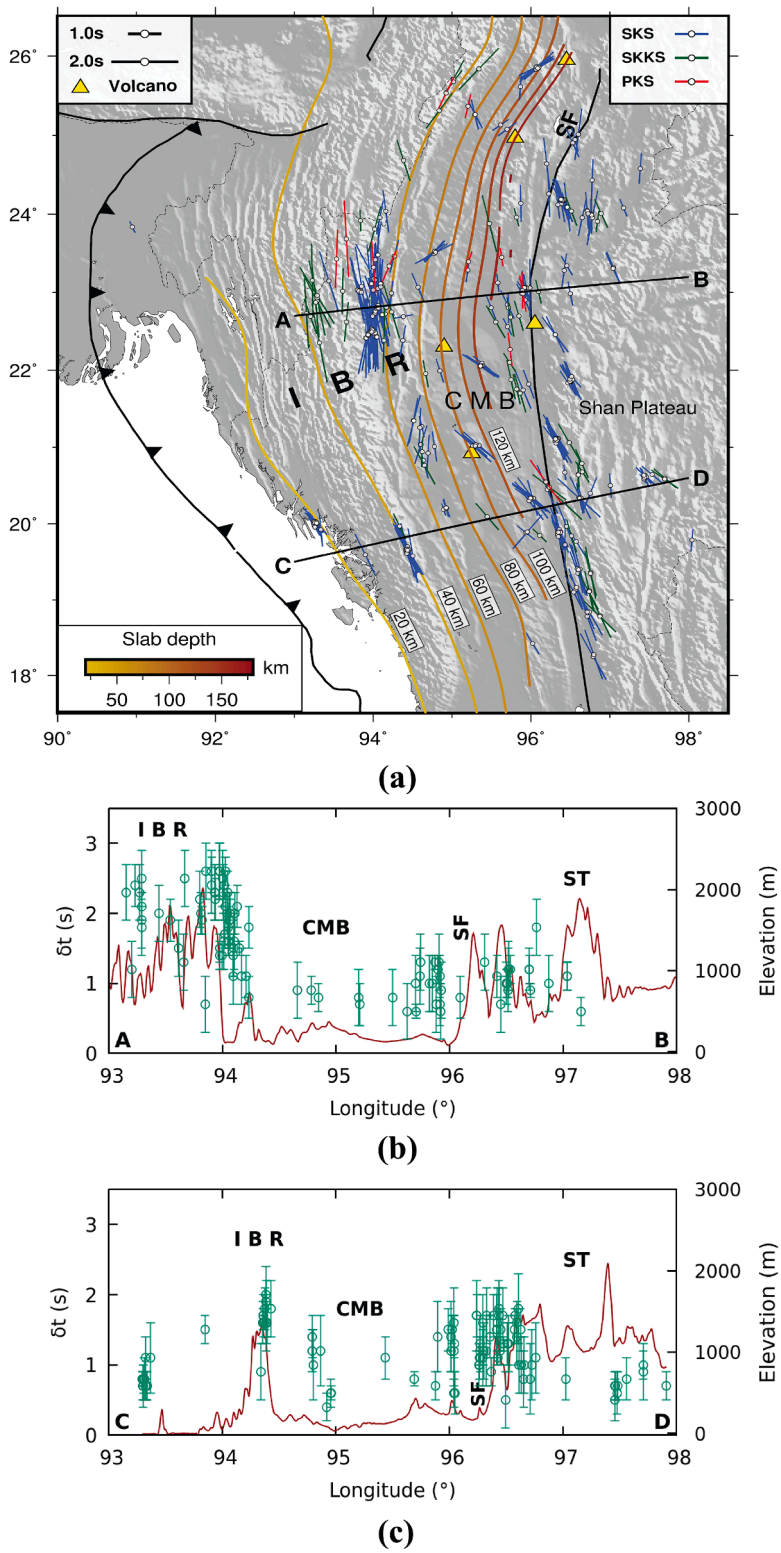

Fig. 6. (a) Individual splitting measurements of the Indo-Burma subduction zone plotted at 210 km depth ray piercing points. Contours represent the slab surface from the SLAB2.0 model at 20 km intervals (Hayes et al., 2018). Yellow triangles show Late Cenozoic volcanoes (from Lee et al., 2016; Searle et al., 2007). Black lines show the locations for profiles; (b) E-W elevation profile with individual splitting lag times in the northern [latitude ~23°N] region; (c) Elevation profile with individual splitting lag times in the southern [latitude ~19°N] region. Profile width is within 1° from the respective line.

exceed ~200 ppm H/Si (Karato et al., 2008).

5.2. *Effect of the Sagaing fault*

We see a sudden increase in lag time close to the SF, especially along the southern portion of the plate boundary (Fig. 6). The dextral motion

along the SF could induce significant shear parallel anisotropy. We note that the offset along the Sagaing Fault is estimated to be 332 ± 128 km (Curray, 2005). Stress-aligned microcrack and shear fabric along the faults could produce anisotropy in the upper crust (Cochran et al., 2006; Crampin, 1990; Crampin and Chastin, 2003; Y. Liu et al., 2008; H. Zhang et al., 2007). The deeper section of the SF is composed of highly deformed metamorphic gneiss and schist of Mesozoic or older origin [e.g., Sagaing Metamorphics] (Bertrand et al., 2001; Thein, 2017). This highly evolved metamorphic fault core of the SF could also increase the strength of the anisotropic fabric. In addition, receiver function studies by Wang et al. (2019) and Zheng et al. (2020) indicate that the SF extends below the Moho in the uppermost mantle. Wu et al. (2021) identified a linear low S wave velocity zone aligned with the Sagaing fault down to 40 km depth. A similar low-velocity anomaly is also observed in other studies (Feng et al., 2020; Wang et al., 2019). The low-velocity uppermost mantle may indicate a warmer than ambient uppermost mantle that would be an ideal place for strain localization and development of a N-S fabric due to the dextral motion. At the continental scale, the SF appears to act as a boundary between the N-S fast direction related to trench-parallel flow and the flow field dominated by E-W fast direction, detailed inspection shows that some measurements immediately to the east of the surface trace of the SF still show predominant N-S direction (Fig. 4& 6). Measurements are sparse in the Shan plateau, but a clear E-W fabric is apparent 100 to 120 km east of the SF.

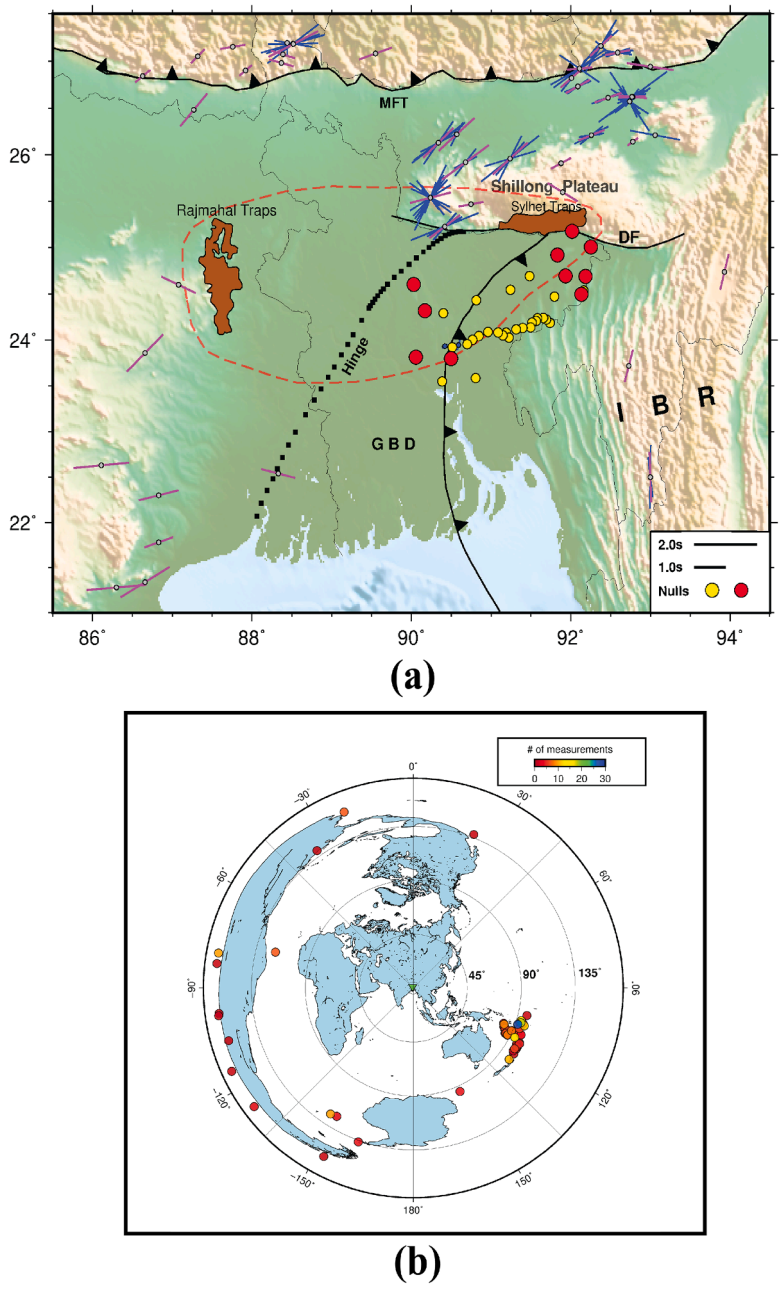

Fig. 7. (a) Nulls and non-null splitting measurements found in Bengal basin in this (yellow) study and previous studies (red) with available shear wave splitting results in surrounding area. The blue and purple bars represent the individual and station average measurements, respectively. Brown polygon shows the surface extent of the basalt flow. Red dotted line encloses the Early Cretaceous Rajmahal-Sylhet plume head (from Kale, 2020). DF – Dauki Fault; (b) Back-azimuth coverage of the events that produced null splitting results in Bengal basin.

5.3. Splitting nulls in the Bengal basin

We have observed null shear wave splitting in the western part of the study area where the outer fold belt of IBR merges with the Bengal basin. Similar null measurements have been observed in previous studies (Fig. 7) where the stations are mostly located in the northeast Sylhet trough and northern GBD (Saikia et al., 2018; Tiwari et al., 2018) areas. When examining the individual splitting measurements of a single event, we also observed a systematic occurrence of nulls in the Bengal basin, while large δt values were observed in the IBR regions (see supplementary material, Fig. S6.2). Since XKS splitting is a path-integrated effect, multiple thin layers of anisotropic media with perpendicular anisotropic orientations will produce apparent null results if their δt values are similar (Menke and Levin, 2003; Saltzer et al., 2000). The western limit of N-S trench parallel flow and the associated transition into an apparent isotropic mantle cannot be determined due to the lack of station coverage; however, the observation of N-S fast directions around 92.5°E (Saikia et al., 2018; Singh et al., 2006) indicates the dominance of trench parallel flow up to the outer portion of the fold and thrust belt beneath the IBR. This slab induced mantle flow most likely extends further west under the Bengal basin. On the other hand, the northwestern Shillong plateau and adjacent areas of the Bengal basin have NE-SW fast axes (Roy et al., 2014; Singh et al., 2007) (Fig. 7). It is surprising that we find this region of no splitting given the likely mantle deformation caused by APM related basal shear or trench parallel sub-slab mantle flow. One possibility is that there is a complex, multiple-layer anisotropy that could make single station measurements appear to be nulls. One way to test this possibility is to look for the presence of residual tangential energy on the corrected transverse components. After careful inspection, we found little evidence of the residual tangential energy that can convincingly prove the presence of multiple anisotropic layers. Of the 264 well-defined null results, only ~7 % of them have residual energy of at least 25 % of the corresponding corrected radial components.

A frozen vertically oriented anisotropic fabric from Kerguelen plume activity is another possible explanation for the lack of splitting in this region. Late Cretaceous (113–118 Ma) Rajmahal and Sylhet traps are considered to be the hotspot trail of this plume activity (Baksi, 1995; Basu et al., 2001; Kent et al., 2002; Ray et al., 2005), or perhaps the initial plume head. Geochemical analysis of major, trace elements and Nd-Sr-Pb isotopes shows the similarities among the Sylhet traps basalt, Rajmahal traps, and the Kerguelen plateau basalt samples (Ghatak and Basu, 2011). Trap basalts are also present in the subsurface stratigraphy in the northwest Bengal basin (Brammer et al., 1995; Khan and Muminullah, 1980). This ~ 800 km wide Kerguelen plume-head under the Bengal basin has also been inferred from the sediment thickness (16–20 km) relative to the crustal thickness (16–19 km), associated high velocities in the lower crust (Singh et al., 2016), and the presence of seaward dipping reflectors (Frielingsdorf et al., 2008). Such large-scale hot injection of plume material could disrupt the ambient mantle flow and produce a vertically orientated LPO fabric. Several plate reconstruction models (Kent et al., 2002; Reeves et al., 2016; Thompson et al., 2019) suggest that the Indian plate had not initiated its fast northward drift during the Kerguelen plume activity, which probably helped to produce such a large plume induced basalt province with vertical lithospheric fabric.

5.4. Mantle flow and the Hainan plume

East of the SF, the fast direction becomes E-W, which prevails over the entire ST and IC blocks (Fig. 8). The development of 2D corner flow due to the viscous coupling between the down-going slab and the overlying wedge could induce the observed E-W fabric (Long and Silver, 2008; Long and Wirth, 2013). Previous studies show (Fig. 2& 8) that the presence of such E-W to NE-SW splitting extends to Vietnam (Bai et al., 2009). The trench normal convergence is likely too slow to produce significant downdip motion of the slab (Mallick et al., 2019) that could develop such extensive corner flow as suggested by some authors (Fan et al., 2021; Kong et al., 2018). Limited arc volcanism implies that there is little slab dehydration and an active corner flow system which transfers fluids to the mantle wedge might be lacking (Hasegawa et al., 2005; Iwamori and Zhao, 2000; J. Wang and Zhao, 2008). Both global

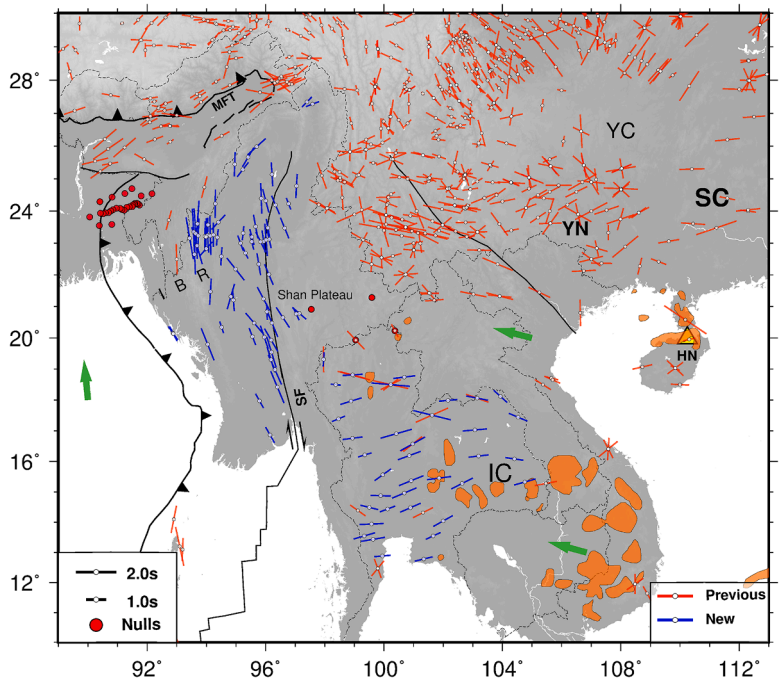

Fig. 8. Available station average splitting measurements integrated with newer results from this study. Previous results are from SWS database (from Barruol et al., 2009). The green arrow shows the direction of the absolute plate motion according to the HS3-NUVEL 1A model. The orange polygon shows the distribution of Late Cenozoic (< 16 Ma) intraplate volcanism. The yellow triangle shows the Hainan volcano. Abbreviations are the same as in Fig. 1.

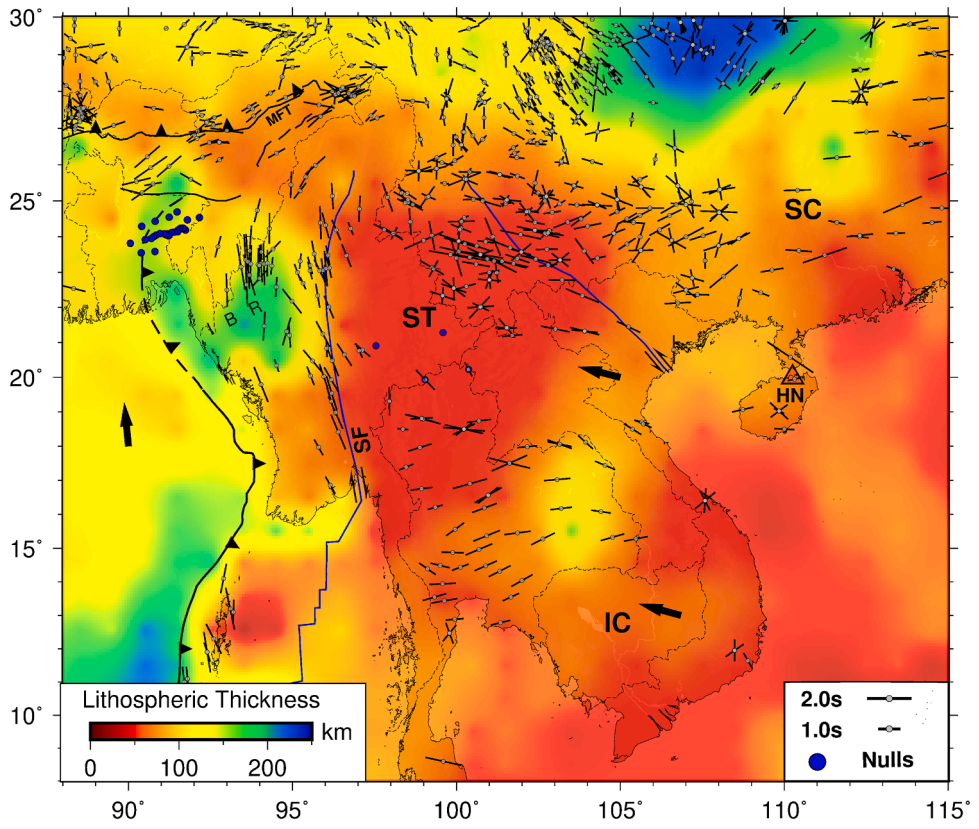

Fig. 9. All station average shear wave splitting measurements of the SE Asia plotted against lithospheric thickness (from Pasyanos et al., 2014).

and regional body wave tomographic models (Koulakov, 2011; Simmons et al., 2010; Wei et al., 2012) reveal that there is very little lithospheric mantle (Fig. 9) across most of southeast Asia, suggesting that the dominant E-W flow is indicative of present-day mantle finite strain patterns. Furthermore, the observed E-W fast direction is also different from the present crustal deformation and strike of the regional tectonic features (Taylor and Yin, 2009). When examining global and regional tomographic models, we also see that the uppermost mantle beneath nearly all of Southeast Asia is dominated by a broad low-velocity zone that can be linked to the Hainan plume beneath the South China sea (Toyokuni et al., 2022; T. Yang et al., 2014; Zhao et al., 2021). Several body wave tomographic models also found a low velocity body beneath the Hainan volcano that reaches the lower mantle (Z. Huang et al., 2015; Lei et al., 2009; Zhao and Liu, 2010). Late Cenozoic intraplate volcanism

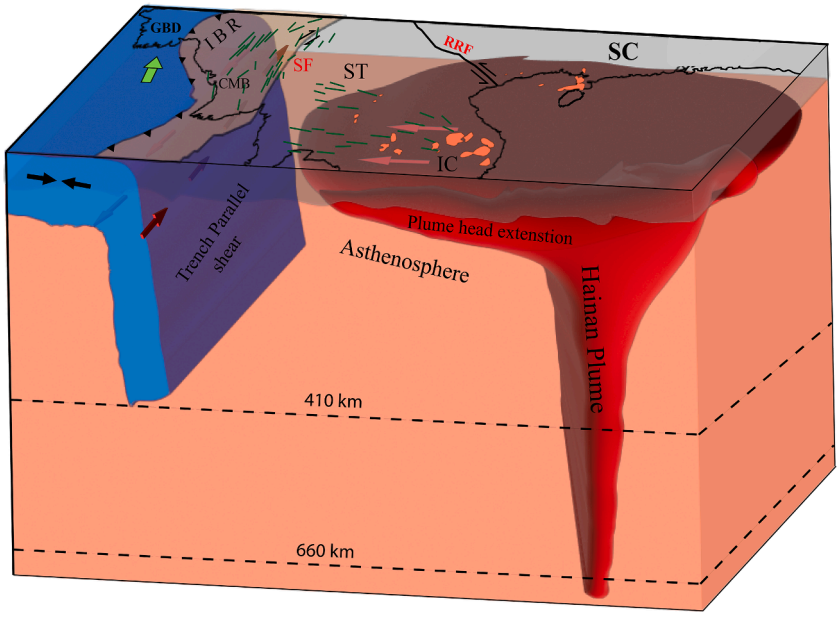

Fig. 10. A conceptual model showing the mantle flow in response to northward motion of the subducting Indian plate and westward plume head migration. Dark green lines show the station average XKS splitting measurements. The red and green arrows show the mantle flow direction and APM direction of the Indian plate, respectively. The orange patches show Late Cenozoic intraplate volcanism.

in Indochina (Fig. 1& 8) with a mixture of a depleted MORB-type and enriched mantle type 2 (EMII) source (Kimura et al., 2018; Yan et al., 2018) is the surface exposure of the westward spreading of the Hainan mantle plume head. The low water content suppressed the melt productivity and upwelling velocity which eventually stalled the plume at the asthenospheric depth (Gu et al., 2019; Kimura et al., 2018), and it probably started extending beneath the lithosphere of the Indochina and South China Sea. The dominant east-west fabric is consistent with asymmetric spreading of the Hainan plume head that has thermally eroded much of the lithospheric mantle. This westward flow appears to extend from Hainan all the way to the Sagaing fault along the eastern edge of the Burma microplate. The Sunda plate is also moving westward according to the hotspot reference frame (HS3-NUVEL-1A) which might have induced the upwelling plume material to be horizontally deflected or sheared in the direction of APM (Walker et al., 2005) towards Indochina (Fig. 10). A similar N-S mantle deformation fabric has also been associated with the Afar plume where the northward movement of the Arabian plate carried the plume head and produced linear N-S basaltic volcanism in the western margin of the Arabian Peninsula (Chang and Van der Lee, 2011; Hansen et al., 2006). The presence of thick lithospheric mantle in the Sichuan basin may act as a barrier to prevent plume material from spreading to the north and resulting in more diverse fast directions near the Sichuan basin (Fig. 9).

5.5. Nulls in Shan plateau

We observed nulls at several stations beneath the ST block in the Shan plateau. Although the extent of the null zone cannot be demarcated precisely due to the sparse station coverage, the clustering of the null measurements (supplementary material, Fig. S6.1) suggests a large region of isotropic seismic velocities structure rather than anomalous stations. One possibility is the initiation of asthenospheric upwelling and the development of vertical olivine strain fabric. In the NW corner of our nulls zone, Singu volcano exhibits an alkaline mafic OIB-type character (Maury et al., 2004; L. Y. Zhang et al., 2020) that also has the signature of enriched isotopes derived from small scale asthenospheric injection. Zhang et al. (2020) proposed a model of asthenospheric upwelling through a slab window around ~22°N to explain the isotropic distribution of the melts. However, without additional geological and geophysical evidence, it is difficult to constrain the existence of such an upwelling, in particular as few regional tomographic models indicate the presence of a hot asthenospheric mantle beneath the Shan plateau (Koulakov, 2011; Wei et al., 2012). The null region could be a transition zone between the S-SW directed extrusion-dominated asthenospheric flow and plume-induced E-W flow. These two competing mantle flow systems could result in no net anisotropy in this area.

6. Conclusion

Measurements of the splitting of core phases (SKS, SKKS, PKS) at 107 stations not previously analyzed indicate the complex nature of the mantle deformation fabric of the highly oblique Indo-Burma subduction system and surrounding regions. The northward Indian motion may have generated trench parallel simple shear around the slab that dominates the entire length of the fore-arc region. Along the Indo-Burma-Ranges, the combination of the sub-slab, slab, and lithospheric fabric results in an observed average lag time of 1.9 s. With the transition up to 100 km east of the Sagaing fault, the E-W fast axes (fluctuating between ENE-WSW and ESE-WNW directions) dominate the rest of the eastern Indochina peninsula. This pattern likely arises from the westward spreading of Hainan plume material under thin lithospheric mantle, probably enhanced by the westward directed absolute plate motion. In the Bengal basin, the absence of splitting is interpreted to reflect the presence of frozen vertical anisotropic fabric associated with Kereguelen plume activity during the Cretaceous rifting episodes of India-Antarctica break up. Additional three-dimensional anisotropic studies and geodynamic modeling are required to unravel the more detailed structure of the mantle deformation field beneath this part of the plate boundary.

CRediT authorship contribution statement

Md Mohimanul Islam: Writing – original draft, Visualization, Validation, Methodology, Investigation, Formal analysis, Conceptualization. **Shengji Wei:** Writing – review & editing, Data curation. **Patricia Persaud:** Writing – review & editing, Funding acquisition. **Michael S. Steckler:** Writing – review & editing, Funding acquisition. **Frederik Tilmann:** Writing – review & editing, Supervision, Data curation. **James Ni:** Writing – review & editing, Conceptualization. **James Gaherty:** Writing – review & editing, Data curation. **Kyaw Moe Oo:** Writing – review & editing, Data curation. **Oo Than:** Data curation. **Yin Myo Min Htwe:** Data curation. **Eric Sandvol:** Writing – review & editing, Supervision, Software, Resources, Project administration, Investigation, Funding acquisition, Data curation.

Declaration of competing interest

The authors declare no financial interest or personal relationship which may be considered as potential competing interest.

Data availability

Part of the datasets are currently restricted. We have uploaded individual windowed waveforms to GitHub, accessible at https://github.com/tnm0110/SWS_data. Please see more information in the supplementary materials.

Acknowledgments

We thank the Earth Observatory of Singapore (EOS), GFZ German Research centre Geosciences, IRIS-DMC, and OHP-DMC for hosting the seismic datasets. We are grateful to colleagues in Bangladesh and Myanmar for their help and support in collecting the BIMA and GFZ datasets, as well as monasteries, regional DMH offices and private landowners for hosting our stations. This research was sponsored by the National Science Foundation (NSF) grant (EAR-1714875, EAR-1714892, EAR-1928360, and EAR-1714651) and the GFZ Expedition Funding. We thank the Geophysical Instrument Pool Potsdam of the GFZ Potsdam for their seismic equipment loan for the 6C network (loan 201814). Splitting measurements were carried out with computer programs developed by co-author Dr. Eric Sandvol (e.g. Gök et al., 2003; León Soto et al., 2012; Sandvol and Hearn, 1994). This code has been tested using several other splitting codes including Splitlab. Many of the graphics in this paper were generated by Generic Mapping Tools [GMT] (Wessel et al., 2019).

Supplementary materials

Supplementary material associated with this article can be found, in the online version, at doi:10.1016/j.epsl.2024.118895.

References

Agius, M.R., Lebedev, S., 2013. Tibetan and Indian lithospheres in the upper mantle beneath Tibet: evidence from broadband surface-wave dispersion. Geochem., Geophy., Geosyst. 14 (10) https://doi.org/10.1002/ggge.20274.

Agius, M.R., Lebedev, S., 2017. Complex, multilayered azimuthal anisotropy beneath Tibet: evidence for co-existing channel flow and pure-shear crustal thickening. Geophys. J. Int. 210 (3) https://doi.org/10.1093/gji/ggx266.

Argus, D.F., Gordon, R.G., Demets, C., 2011. Geologically current motion of 56 plates relative to the no-net-rotation reference frame. Geochemistry, Geophysics, Geosystems 12 (11). https://doi.org/10.1029/2011GC003751.

Bai, L., Iidaka, T., Kawakatsu, H., Morita, Y., Dzung, N.Q., 2009. Upper mantle anisotropy beneath Indochina block and adjacent regions from shear-wave splitting analysis of Vietnam broadband seismograph array data. Phy.e Earth Planet. Inter. 176 (1–2) https://doi.org/10.1016/j.pepi.2009.03.008.

Baksi, A.K., 1995. Petrogenesis and timing of volcanism in the Rajmahal flood basalt province, northeastern India. Chem. Geol. 121 (1–4) https://doi.org/10.1016/0009-2541(94)00124-Q.

Barruol, G., Wuestefeld, A., Bokelmann, G., 2009. SKS-Splitting-database. Université de Montpellier, Laboratoire Géosciences.

Basu, A.R., Weaver, K.L., Sengupta, S., 2001. A plume head and tail in the Bengal basin and bay of Bengal: Rajmahal and Sylhet traps with surrounding Alkalic volcanism and the Ninetyeast ridge. In: AGU Fall Meeting Abstracts, 2001, pp. V12A–0950. https://ui.adsabs.harvard.edu/abs/2001AGUFM.V12A0950B.

Bertrand, G., Rangin, C., 2003. Tectonics of the western margin of the Shan plateau (central Myanmar): implication for the India-Indochin oblique convergence since the Oligocene. J. Asian Earth. Sci. 21 (10) https://doi.org/10.1016/S1367-9120(02)00183-9.

Bertrand, G., Rangin, C., Maluski, H., Bellon, H., 2001. Diachronous cooling along the mogok metamorphic belt (Shan scarp, Myanmar): the trace of the northward migration of the Indian syntaxis. J. Asian Earth. Sci. 19 (5) https://doi.org/10.1016/S1367-9120(00)00061-4.

Betka, P.M., Seeber, L., Thomson, S.N., Steckler, M.S., Sincavage, R., Zoramthara, C., 2018. Slip-partitioning above a shallow, weak décollement beneath the Indo-Burman accretionary prism. Earth Planet. Sci. Lett. 503 https://doi.org/10.1016/j.epsl.2018.09.003.

Brammer, H., Khan, F.H., Reimann, K.U., 1995. Geology of Bangladesh. Geogr. J. 161 (1) https://doi.org/10.2307/3059933.

Chang, S.J., Van der Lee, S., 2011. Mantle plumes and associated flow beneath Arabia and East Africa. Earth Planet. Sci. Lett. 302 (3), 448–454. https://doi.org/10.1016/j.epsl.2010.12.050.

Chang, L., Flesch, L.M., Wang, C.Y., Ding, Z., 2015. Vertical coherence of deformation in lithosphere in the eastern Himalayan syntaxis using GPS, Quaternary fault slip rates, and shear wave splitting data. Geophys. Res. Lett. 42 (14) https://doi.org/10.1002/2015GL064568.

Christensen, N.I., 1984. The magnitude, symmetry and origin of upper mantle anisotropy based on fabric analyses of ultramafic tectonites. Geophys. J. Royal Astronom. Soc. 76 (1) https://doi.org/10.1111/j.1365-246X.1984.tb05025.x.

Cochran, E.S., Li, Y.G., Vidale, J.E., 2006. Anisotropy in the shallow crust observed around the San Andreas fault before and after the 2004 M 6.0 parkfield earthquake. Bullet. Seismolog. Soc. Am. 96 (4 B) https://doi.org/10.1785/0120050804.

Crampin, S., Chastin, S., 2003. A review of shear wave splitting in the crack-critical crust. Geophys. J. Int. 155 (1) https://doi.org/10.1046/j.1365-246X.2003.02037.x.

Crampin, S., 1990. The scattering of shear-waves in the crust. Pure Appl. Geophy. PAGEOPH 132 (1–2). https://doi.org/10.1007/BF00874358.

Curray, J.R., 2005. Tectonics and history of the Andaman Sea region. J. Asian Earth. Sci. 25 (1) https://doi.org/10.1016/j.jseaes.2004.09.001.

Dasgupta, S., Mukhopadhyay, M., Bhattacharya, A., Jana, T.K., 2003. The geometry of the Burmese-Andaman subducting lithosphere. J. Seismol. 7 (2), 155–174. https://doi.org/10.1023/A:1023520105384.

Department of Meteorology and Hydrology - National Earthquake Data Center, 2016. *Myanmar National Seismic Network [Data set]*. International Federation of Digital Seismograph Networks. https://doi.org/10.7914/SN/MM.

Devachandra, M., Kundu, B., Catherine, J., Kumar, A., Gahalaut, V.K., 2014. Global Positioning System (GPS) measurements of crustal deformation across the frontal eastern Himalayan syntaxis and seismic-hazard assessment. Bull. Seismolog. Soc. Am. 104 (3) https://doi.org/10.1785/0120130290.

Dubey, A.K., Singh, A., Kumar, M.R., Jana, N., Sarkar, S., Saikia, D., Singh, C., 2022. Tomographic imaging of the plate geometry beneath the arunachal himalaya and burmese subduction zones. Geophys. Res. Lett. 49 (8) https://doi.org/10.1029/2022GL098331.

Fan, E., He, Y., Ai, Y., Gao, S.S., Liu, K.H., Jiang, M., Hou, G., Mon, C.T., Thant, M., Sein, K., 2021. Seismic anisotropy and mantle flow constrained by shear wave splitting in central Myanmar. Solid Earth 126 (10). https://doi.org/10.1029/2021JB022144.

Fan, E., Ai, Y., Gao, S.S., He, Y., Liu, K.H., Jiang, M., Hou, G., Yang, S., Mon, C.T., Thant, M., Sein, K., 2024. Mantle flow and olivine fabric transition in the Myanmar continental subduction zone. Geology. 52 (4) https://doi.org/10.1130/G51698.1.

Feng, M., An, M., Mechie, J., Zhao, W., Xue, G., Su, H., 2020. Lithospheric structures of and tectonic implications for the central-east Tibetan plateau inferred from joint tomography of receiver functions and surface waves. Geophys. J. Int. 223 (3) https://doi.org/10.1093/gji/ggaa403.

Fitch, T.J., 1972. Plate convergence, transcurrent faults, and internal deformation adjacent to Southeast Asia and the western Pacific. J. Geophys. Res. 77 (23) https://doi.org/10.1029/jb077i023p04432.

Frielingsdorf, J., Aminul Islam, S., Block, M., Mizanur Rahman, M., Golam Rabbani, M., 2008. Tectonic subsidence modelling and Gondwana source rock hydrocarbon potential, Northwest Bangladesh Modelling of Kuchma, Singra and Hazipur wells. Mar. Pet. Geol. 25 (6) https://doi.org/10.1016/j.marpetgeo.2007.07.013.

Gök, R., Ni, J.F., West, M., Sandvol, E., Wilson, D., Aster, R., Baldridge, W.S., Grand, S., Gao, W., Tillmann, F., Semken, S., 2003. Shear wave splitting and mantle flow beneath LA RISTRA. Geophys. Res. Lett. 30 (12) https://doi.org/10.1029/2002GL016616.

Gan, W., Zhang, P., Shen, Z.K., Niu, Z., Wang, M., Wan, Y., Zhou, D., Cheng, J., 2007. Present-day crustal motion within the Tibetan Plateau inferred from GPS measurements. Solid Earth 112 (8). https://doi.org/10.1029/2005JB004120.

Gao, S.S., Liu, K.H., 2012. AnisDep: a FORTRAN program for the estimation of the depth of anisotropy using spatial coherency of shear-wave splitting parameters. Comput. Geosci. 49 https://doi.org/10.1016/j.cageo.2012.01.020.

Ghatak, A., Basu, A.R., 2011. Vestiges of the Kerguelen plume in the Sylhet Traps, northeastern India. Earth Planet. Sci. Lett. 308 (1–2) https://doi.org/10.1016/j.epsl.2011.05.023.

Gripp, A.E., Gordon, R.G., 2002. Young tracks of hotspots and current plate velocities. Geophys. J. Int. 150 (2) https://doi.org/10.1046/j.1365-246X.2002.01627.x.

Gu, X.Y., Wang, P.Y., Kuritani, T., Hanski, E., Xia, Q.K., Wang, Q.Y., 2019. Low water content in the mantle source of the Hainan plume as a factor inhibiting the formation of a large igneous province. Earth Planet. Sci. Lett. 515 https://doi.org/10.1016/j.epsl.2019.03.034.

Gupta, T.D., Riguzzi, F., Dasgupta, S., Mukhopadhyay, B., Roy, S., Sharma, S., 2015. Kinematics and strain rates of the Eastern Himalayan Syntaxis from new GPS campaigns in Northeast India. Tectonophysics. 655 https://doi.org/10.1016/j.tecto.2015.04.017.

Hansen, S., Schwartz, S., Al-Amri, A., Rodgers, A., 2006. Combined plate motion and density-driven flow in the asthenosphere beneath Saudi Arabia: evidence from shear-wave splitting and seismic anisotropy. Geology. 34 (10) https://doi.org/10.1130/G22713.1.

Hasegawa, A., Nakajima, J., Umino, N., Miura, S., 2005. Deep structure of the northeastern Japan arc and its implications for crustal deformation and shallow seismic activity. Tectonophysics. 403 (1–4) https://doi.org/10.1016/j.tecto.2005.03.018.

Hayes, G.P., Moore, G.L., Portner, D.E., Hearne, M., Flamme, H., Furtney, M., Smoczyk, G.M., 2018. Slab2, a comprehensive subduction zone geometry model. Science) 362 (6410), 58–61. https://doi.org/10.1126/science.aat4723.

Huang, J., Zhao, D., 2006. High-resolution mantle tomography of China and surrounding regions. Solid Earth 111 (B9). https://doi.org/10.1029/2005JB004066.

Huang, Z., Wang, L., Xu, M., Liu, J., Mi, N., Liu, S., 2007. Shear wave splitting across the Ailao Shan-Red River fault zone, SW China. Geophys. Res. Lett. 34 (20) https://doi.org/10.1029/2007GL031236.

Huang, Z., Zhao, D., Wang, L., 2015. P wave tomography and anisotropy beneath Southeast Asia: insight into mantle dynamics. Solid Earth 120 (7). https://doi.org/10.1002/2015JB012098.

Hurukawa, N., Tun, P.P., Shibazaki, B., 2012. Detailed geometry of the subducting Indian Plate beneath the Burma Plate and subcrustal seismicity in the Burma Plate derived from joint hypocenter relocation. Earth, Planets Space 64 (4). https://doi.org/10.5047/eps.2011.10.011.

Iwamori, H., Zhao, D., 2000. Melting and seismic structure beneath the Northeast Japan Arc. Geophys. Res. Lett. 27 (3) https://doi.org/10.1029/1999 gl010917.

Jolivet, L., Faccenna, C., Becker, T., Tesauro, M., Sternai, P., Bouilhol, P., 2018. Mantle Flow and Deforming Continents: from India-Asia Convergence to Pacific Subduction. Tectonics. 37 (9) https://doi.org/10.1029/2018TC005036.

Kale, V.S., 2020. Cretaceous volcanism in peninsular India: rajmahal–sylhet and deccan traps. Springer Geology. https://doi.org/10.1007/978-3-030-15989-4_8.

Karato, S.I., Jung, H., Katayama, I., Skemer, P., 2008. Geodynamic significance of seismic anisotropy of the upper mantle: new insights from laboratory studies. Annu Rev. Earth. Planet. Sci. 36 https://doi.org/10.1146/annurev.earth.36.031207.124120.

Kayal, J.R., 2008. Microearthquake seismology and seismotectonics of South Asia. Microearthquake Seismology and Seismotectonics of South Asia. https://doi.org/10.1007/978-1-4020-8180-4.

Keep, M., Schellart, W.P., 2012. Introduction to the thematic issue on the evolution and dynamics of the Indo-Australian plate. Austral. J. Earth Sci. 59 (6) https://doi.org/10.1080/08120099.2012.708360.

Kent, R.W., Pringle, M.S., Müller, R.D., Saunders, A.D., Ghose, N.C., 2002. 40Ar/39Ar geochronology of the Rajmahal Basalts, India, and their relationship to the Kerguelen plateau. J. Petrol. 43 (7) https://doi.org/10.1093/petrology/43.7.1141.

Khan, M.R., Muminullah, M., 1980. Stratigraphy of Bangladesh. Petroleum and Mineral Resources of Bangladesh: Seminar and Exhibition, pp. 35–40.

Khin, K., Zaw, K., Aung, L.T., 2017. Geological and tectonic evolution of the Indo-Myanmar Ranges (IMR) in the Myanmar region. Geolog. Soc. Memoir 48 (1). https://doi.org/10.1144/M48.4.

Kimura, J.I., Sakuyama, T., Miyazaki, T., Vaglarov, B.S., Fukao, Y., Stern, R.J., 2018. Plume-stagnant slab-lithosphere interactions: origin of the late Cenozoic intra-plate basalts on the East Eurasia margin. Lithos. 300–301 https://doi.org/10.1016/j.lithos.2017.12.003.

Kong, F., Wu, J., Liu, L., Liu, K.H., Song, J., Li, J., Gao, S.S., 2018. Azimuthal anisotropy and mantle flow underneath the southeastern Tibetan Plateau and northern Indochina Peninsula revealed by shear wave splitting analyses. Tectonophysics. 747–748, 68–78. https://doi.org/10.1016/j.tecto.2018.09.013.

Koulakov, I., 2011. High-frequency P and S velocity anomalies in the upper mantle beneath Asia from inversion of worldwide traveltime data. Solid Earth 116 (4). https://doi.org/10.1029/2010JB007938.

Kreemer, C., Blewitt, G., Klein, E.C., 2014. A geodetic plate motion and Global Strain Rate Model. Geochem., Geophys., Geosyst. 15 (10) https://doi.org/10.1002/2014GC005407.

Le Pichon, X., Fournier, M., Jolivet, L., 1992. Kinematics, topography, shortening, and extrusion in the India-Eurasia collision. Tectonics. 11 (6) https://doi.org/10.1029/92TC01566.

Lee, H.Y., Chung, S.L., Yang, H.M., 2016. Late Cenozoic volcanism in central Myanmar: geochemical characteristics and geodynamic significance. Lithos. 245 https://doi.org/10.1016/j.lithos.2015.09.018.

Lei, J., Zhao, D., 2016. Teleseismic P-wave tomography and mantle dynamics beneath Eastern Tibet. Geochem.y, Geophys., Geosyst. 17 (5) https://doi.org/10.1002/2016GC006262.

Lei, J., Zhao, D., Steinberger, B., Wu, B., Shen, F., Li, Z., 2009. New seismic constraints on the upper mantle structure of the Hainan plume. Phys. Earth Planet. Interiors 173 (1–2). https://doi.org/10.1016/j.pepi.2008.10.013.
Lev, E., Long, M.D., van der Hilst, R.D, 2006. Seismic anisotropy in Eastern Tibet from shear wave splitting reveals changes in lithospheric deformation. Earth Planet. Sci. Lett. 251 (3–4) https://doi.org/10.1016/j.epsl.2006.09.018.
Li, C., van der Hilst, R.D., Meltzer, A.S., Engdahl, E.R., 2008. Subduction of the Indian lithosphere beneath the Tibetan Plateau and Burma. Earth Planet. Sci. Lett. 274 (1–2) https://doi.org/10.1016/j.epsl.2008.07.016.
Li, S., Advokaat, E.L., van Hinsbergen, D.J.J., Koymans, M., Deng, C., Zhu, R., 2017. Paleomagnetic constraints on the Mesozoic-Cenozoic paleolatitudinal and rotational history of Indochina and South China: review and updated kinematic reconstruction. Earth. Sci. Rev. 171 https://doi.org/10.1016/j.earscirev.2017.05.007.
Liang, S., Gan, W., Shen, C., Xiao, G., Liu, J., Chen, W., Ding, X., Zhou, D., 2013. Three-dimensional velocity field of present-day crustal motion of the Tibetan Plateau derived from GPS measurements. Solid Earth 118 (10). https://doi.org/10.1002/2013JB010503.
Liu, K.H., Gao, S.S., 2011. Estimation of the depth of anisotropy using spatial coherency of shear-wave splitting parameters. Bull. Seismolog. Soc. Am 101 (5). https://doi.org/10.1785/0120100258.
Liu, Y., Zhang, H., Thurber, C., Roecker, S., 2008. Shear wave anisotropy in the crust around the San Andreas fault near Parkfield: spatial and temporal analysis. Geophys. J. Int. 172 (3) https://doi.org/10.1111/j.1365-246X.2007.03618.x.
Liu, L., Gao, S.S., Liu, K.H., Li, S., Tong, S., Kong, F., 2019. Toroidal mantle flow induced by slab subduction and rollback beneath the eastern himalayan syntaxis and adjacent areas. Geophys. Res. Lett. 46 (20) https://doi.org/10.1029/2019GL084961.
Long, M.D., Becker, T.W., 2010. Mantle dynamics and seismic anisotropy. Earth Planet. Sci. Lett. 297 (3–4) https://doi.org/10.1016/j.epsl.2010.06.036.
Long, M.D., Silver, P.G., 2008. The subduction zone flow field from seismic anisotropy: a global view. Science 319 (5861). https://doi.org/10.1126/science.1150809.
Long, M.D., Silver, P.G., 2009. Shear wave splitting and mantle anisotropy: measurements, interpretations, and new directions. Surv. Geophys. 30 (4–5) https://doi.org/10.1007/s10712-009-9075-1. Issues.
Long, M.D., Wirth, E.A., 2013. Mantle flow in subduction systems: the mantle wedge flow field and implications for wedge processes. Solid Earth 118 (2). https://doi.org/10.1002/jgrb.50063.
Mallick, R., Lindsey, E.O., Feng, L., Hubbard, J., Banerjee, P., Hill, E.M., 2019. Active convergence of the india-burma-sunda plates revealed by a new continuous GPS network. Solid Earth 124 (3). https://doi.org/10.1029/2018JB016480.
Marechal, A., Mazzotti, S., Cattin, R., Cazes, G., Vernant, P., Drukpa, D., Thinley, K., Tarayoun, A., Le Roux-Mallouf, R., Thapa, B.B., Pelgay, P., Gyeltshen, J., Doerflinger, E., Gautier, S., 2016. Evidence of interseismic coupling variations along the Bhutan Himalayan arc from new GPS data. Geophys. Res. Lett. 43 (24) https://doi.org/10.1002/2016GL071163.
Maurin, T., Rangin, C., 2009. Structure and kinematics of the Indo-Burmese Wedge: recent and fast growth of the outer wedge. Tectonics. 28 (2) https://doi.org/10.1029/2008TC002276.
Maury, R.C., Pubellier, M., Rangin, C., Wulput, L., Cotten, J., Socquet, A., Bellon, H., Guillaud, J.P., Htun, H.M., 2004. Quaternary calc-alkaline and alkaline volcanism in an hyper-oblique convergence setting, central Myanmar and western Yunnan. Bulletin de La Societe Geologique de France 175 (5). https://doi.org/10.2113/175.5.461.
McNamara, D.E., Owens, T.J., Silver, P.G., Wu, F.T., 1994. Shear wave anisotropy beneath the Tibetan Plateau. Solid Earth 99 (B7). https://doi.org/10.1029/93jb03406.
Menke, W., Levin, V., 2003. The cross-convolution method for interpreting SKS splitting observations, with application to one and two-layer anisotropic earth models. Geophys. J. Int. 154 (2) https://doi.org/10.1046/j.1365-246X.2003.01937.x.
Metcalfe, I., 2011. Tectonic framework and Phanerozoic evolution of Sundaland. Gondwana Res. 19 (1) https://doi.org/10.1016/j.gr.2010.02.016.
Metcalfe, I., 2013. Gondwana dispersion and Asian accretion: tectonic and palaeogeographic evolution of eastern Tethys. J. Asian Earth. Sci. 66 https://doi.org/10.1016/j.jseaes.2012.12.020.
Mitchell, A.H.G., 1993. Cretaceous-Cenozoic tectonic events in the western Myanmar (Burma)- Assam region. J. - Geolog. Soc. 150 (6) https://doi.org/10.1144/gsjgs.150.6.1089.
Molnar, P., Tapponnier, P., 1975. Cenozoic tectonics of asia: effects of a continental collision: features of recent continental tectonics in asia can be interpreted as results of the india-eurasia collision. Science 189 (4201). https://doi.org/10.1126/science.189.4201.419.
Mon, C.T., Gong, X., Wen, Y., Jiang, M., Chen, Q.F., Zhang, M., Hou, G., Thant, M., Sein, K., He, Y., 2020. Insight into major active faults in central myanmar and the related geodynamic sources. Geophys. Res. Lett. 47 (8) https://doi.org/10.1029/2019GL086236.
Morley, C.K., Arboit, F., 2019. Dating the onset of motion on the Sagaing fault: evidence from detrital zircon and titanite U-Pb geochronology from the North Minwun Basin, Myanmar. Geology. 47 (6) https://doi.org/10.1130/G46321.1.
Morley, C.K., 2002. A tectonic model for the Tertiary evolution of strike-slip faults and rift basins in SE Asia. Tectonophysics. 347 (4) https://doi.org/10.1016/S0040-1951(02)00061-6.
Morley, C.K., 2007. Variations in Late Cenozoic-Recent strike-slip and oblique-extensional geometries, within Indochina: the influence of pre-existing fabrics. J. Struct. Geol. 29 (1) https://doi.org/10.1016/j.jsg.2006.07.003.
Morley, C.K., 2017. Syn-kinematic sedimentation at a releasing splay in the northern Minwun Ranges, Sagaing Fault zone, Myanmar: significance for fault timing and displacement. Basin Res. 29 https://doi.org/10.1111/bre.12201.
Najman, Y., Sobel, E.R., Millar, I., Stockli, D.F., Govin, G., Lisker, F., Garzanti, E., Limonta, M., Vezzoli, G., Copley, A., Zhang, P., Szymanski, E., Kahn, A., 2020. The exhumation of the Indo-Burman Ranges, Myanmar. Earth Planet. Sci. Lett. 530 https://doi.org/10.1016/j.epsl.2019.115948.
Nakakuki, T., Mura, E., 2013. Dynamics of slab rollback and induced back-arc basin formation. Earth Planet. Sci. Lett. 361 https://doi.org/10.1016/j.epsl.2012.10.031.
Ng, S.W.P., Whitehouse, M.J., Searle, M.P., Robb, L.J., Ghani, A.A., Chung, S.L., Oliver, G.J.H., Sone, M., Gardiner, N.J., Roselee, M.H., 2015. Petrogenesis of Malaysian granitoids in the Southeast Asian tin belt: part 2. U-Pb zircon geochronology and tectonic model. Bull. Geolog. Soci.f Am. 127 (9–10) https://doi.org/10.1130/B31214.1.
Ni, J.F., Guzman-Speziale, M., Bevis, M., Holt, W.E., Wallace, T.C., Seager, W.R., 1989. Accretionary tectonics of Burma and the three-dimensional geometry of the Burma subduction zone. Geology. 17 (1) https://doi.org/10.1130/0091-7613(1989)017<0068:ATOBAT>2.3.CO;2.
Oryan, B., Betka, P.M., Steckler, M.S., Nooner, S.L., Lindsey, E.O., Mondal, D., Mathews, A.M., Akhter, S.H., Singha, S., Than, O., 2023. New GNSS and geological data from the indo-burman subduction zone indicate active convergence on both a locked megathrust and the Kabaw Fault. Solid Earth 128 (4), e2022JB025550. https://doi.org/10.1029/2022JB025550.
Pasyanos, M.E., Masters, T.G., Laske, G., Ma, Z., 2014. LITHO1.0: an updated crust and lithospheric model of the Earth. Solid Earth 119 (3). https://doi.org/10.1002/2013JB010626.
Prelević, D., Akal, C., Romer, R.L., Mertz-Kraus, R., Helvaci, C., 2015. Magmatic response to slab tearing: constraints from the afyon alkaline volcanic complex, Western Turkey. J. Petrol. 56 (3) https://doi.org/10.1093/petrology/egv008.
Rao, N.P., Kalpna, 2005. Deformation of the subducted Indian lithospheric slab in the Burmese arc. Geophys. Res. Lett. 32 (5) https://doi.org/10.1029/2004GL022034.
Ray, J.S., Pattanayak, S.K., Pande, K., 2005. Rapid emplacement of the Kerguelen plume-related Sylhet Traps, eastern India: evidence from 40Ar-39Ar geochronology. Geophys. Res. Lett. 32 (10) https://doi.org/10.1029/2005GL022586.
Reeves, C.V., Teasdale, J.P., Mahanjane, E.S., 2016. Insight into the eastern margin of Africa from a new tectonic model of the Indian Ocean. Geol. Soc. Spec. Publ. 431 (1) https://doi.org/10.1144/SP431.12.
Replumaz, A., Tapponnier, P., 2003. Reconstruction of the deformed collision zone Between India and Asia by backward motion of lithospheric blocks. Solid Earth 108 (B6). https://doi.org/10.1029/2001jb000661.
Richter, B., Fuller, M., 1996. Palaeomagnetism of the Sibumasu and Indochina blocks: implications for the extrusion tectonic model. Geol. Soc. Spec. Publ. 106 https://doi.org/10.1144/GSL.SP.1996.106.01.13.
Roy, S.K., Ravi Kumar, M., D, S, 2014. Upper and lower mantle anisotropy inferred from comprehensive SKS and SKKS splitting measurements from India. Earth Planet. Sci. Lett. 392 https://doi.org/10.1016/j.epsl.2014.02.012.
Russo, R.M., 2012. Source-side shear-wave splitting and upper-mantle flow beneath the Arakan slab, India-Asia-Sundalind triple junction. Geosphere 8 (1). https://doi.org/10.1130/GES00534.1.
Saikia, D., Kumar, M.R., Singh, A., Roy, S.K., Raju, P.S., Lyngdoh, A.C., 2018. Mantle Deformation in the Eastern Himalaya, Burmese Arc and Adjoining Regions. Geochem., Geophys., Geosyst. 19 (11), 4420–4432. https://doi.org/10.1029/2018GC007691.
Saltzer, R.L., Gaherty, J.B., Jordan, T.H., 2000. How are vertical shear wave splitting measurements affected by variations in the orientation of azimuthal anisotropy with depth? Geophys. J. Int. 141 (2) https://doi.org/10.1046/j.1365-246X.2000.00088.x.
Sandvol, E., Hearn, T., 1994. Bootstrapping shear-wave splitting errors. Bull. - Seismolog. Soc. Am. 84 (6) https://doi.org/10.1785/bssa0840061971.
Sandvol, E., Gaherty, J., Steckler, M., Persaud, P., 2018. Tripartite-BIMA (Bangladesh-India-Myanmar Array) [Data Set]. International Federation of Digital Seismograph Networks. https://doi.org/10.7914/SN/XR_2018.
Sato, K., Liu, Y., Wang, Y., Yokoyama, M., Yoshioka, S., Yang, Z., Otofuji, Y.ichiro., 2007. Paleomagnetic study of Cretaceous rocks from Pu'er, western Yunnan, China: evidence of internal deformation of the Indochina block. Earth Planet. Sci. Lett. 258 (1–2) https://doi.org/10.1016/j.epsl.2007.02.043.
Satyabala, S.P., 2003. Oblique plate convergence in the Indo-Burma (Myanmar) subduction region. Pure Appl. Geophys. 160 (9) https://doi.org/10.1007/s00024-003-2378-0.
Savage, M.S., 1999. Seismic anisotropy and mantle deformation: what have we learned from shear wave splitting? Rev. Geophys. 37 (1) https://doi.org/10.1029/98RG02075.
Schellart, W.P., Moresi, L., 2013. A new driving mechanism for backarc extension and backarc shortening through slab sinking induced toroidal and poloidal mantle flow: results from dynamic subduction models with an overriding plate. Solid Earth 118 (6). https://doi.org/10.1002/jgrb.50173.
Searle, M.P., Morley, C.K., 2011. Tectonic and thermal evolution of Thailand in the regional context of SE Asia. The Geology of Thailand. The Geological Society of London, pp. 539–571. https://doi.org/10.1144/GOTH.20.
Searle, M.P., Noble, S.R., Cottle, J.M., Waters, D.J., Mitchell, A.H.G., Hlaing, T., Horstwood, M.S.A., 2007. Tectonic evolution of the Mogok metamorphic belt, Burma (Myanmar) constrained by U-Th-Pb dating of metamorphic and magmatic rocks. Tectonics 26 (3). https://doi.org/10.1029/2006TC002083.
Searle, M.P., Whitehouse, M.J., Robb, L.J., Ghani, A.A., Hutchison, C.S., Sone, M., Ng, S. W.P., Roselee, M.H., Chung, S.L., Oliver, G.J.H., 2012. Tectonic evolution of the Sibumasu-Indochina terrane collision zone in Thailand and Malaysia: constraints

from new U-Pb zircon chronology of SE Asian tin granitoids. J. Geol. Soc. London. 169 (4) https://doi.org/10.1144/0016-76492011-107.
Shi, H., Li, T., Zhang, R., Zhang, G., Yang, H., 2020. Imaging of the Upper Mantle Beneath Southeast Asia: constrained by teleseismic P-wave tomography. Remote Sens. 12 (18) https://doi.org/10.3390/RS12182975.
Silver, P.G., Chan, W.W., 1991. Shear wave splitting and subcontinental mantle deformation. J. Geophys. Res. 96 (B10) https://doi.org/10.1029/91jb00899.
Silver, P.G., Savage, M.K., 1994. The interpretation of shear-wave splitting parameters in the presence of two anisotropic layers. Geophys. J. Int. 119 (3) https://doi.org/10.1111/j.1365-246X.1994.tb04027.x.
Silver, P.G., 1996. Seismic anisotropy beneath the continents: probing the depths of geology. Annu Rev. Earth. Planet. Sci. 24 https://doi.org/10.1146/annurev.earth.24.1.385.
Simmons, N.A., Forte, A.M., Boschi, L., Grand, S.P., 2010. GyPSuM: a joint tomographic model of mantle density and seismic wave speeds. Solid Earth 115 (12). https://doi.org/10.1029/2010JB007631.
Singh, A., Kumar, M.R., Raju, P.S., Ramesh, D.S., 2006. Shear wave anisotropy of the northeast Indian lithosphere. Geophys. Res. Lett. 33 (16) https://doi.org/10.1029/2006GL026106.
Singh, A., Kumar, M.R., Raju, P.S., 2007. Mantle deformation in Sikkim and adjoining Himalaya: evidences for a complex flow pattern. Phys. Earth Planet. Inter. 164 (3–4) https://doi.org/10.1016/j.pepi.2007.07.003.
Singh, A., Bhushan, K., Singh, C., Steckler, M.S., Akhter, S.H., Seeber, L., Kim, W.Y., Tiwari, A.K., Biswas, R., 2016. Crustal structure and tectonics of Bangladesh: new constraints from inversion of receiver functions. Tectonophysics. 680 https://doi.org/10.1016/j.tecto.2016.04.046.
Socquet, A., Pubellier, M., 2005. Cenozoic deformation in western Yunnan (China-Myanmar border). J. Asian Earth. Sci. 24 (4) https://doi.org/10.1016/j.jseaes.2004.03.006.
Sol, S., Meltzer, A., Bürgmann, R., van der Hilst, R.D., King, R., Chen, Z., Koons, P.O., Lev, E., Liu, Y.P., Zeitler, P.K., Zhang, X., Zhang, J., Zurek, B., 2007. Geodynamics of the southeastern Tibetan Plateau from seismic anisotropy and geodesy. Geology. 35 (6), 563–566. https://doi.org/10.1130/G23408A.1.
Sone, M., Metcalfe, I., 2008. Parallel Tethyan sutures in mainland Southeast Asia: new insights for Palaeo-Tethys closure and implications for the Indosinian orogeny. Comptes Rendus - Geoscience 340 (2–3). https://doi.org/10.1016/j.crte.2007.09.008.
León Soto, G., Sandvol, E., Ni, J.F., Flesch, L., Hearn, T.M., Tilmann, F., Chen, J., Brown, L.D, 2012. Significant and vertically coherent seismic anisotropy beneath eastern Tibet. Solid Earth 117 (5). https://doi.org/10.1029/2011JB008919.
Steckler, M.S., Mondal, D.R., Akhter, S.H., Seeber, L., Feng, L., Gale, J., Hill, E.M., Howe, M., 2016. Locked and loading megathrust linked to active subduction beneath the Indo-Burman Ranges. Nat. Geosci. 9 (8) https://doi.org/10.1038/ngeo2760.
Stork, A.L., Selby, N.D., Heyburn, R., Searle, M.P., 2008. Accurate relative earthquake hypocenters reveal structure of the Burma subduction zone. Bull. Seismolog.l Soc. America 98 (6). https://doi.org/10.1785/0120080088.
Takemoto, K., Sato, S., Chanthavichith, K., Inthavong, T., Inokuchi, H., Fujihara, M., Zaman, H., Yang, Z., Yokoyama, M., Iwamoto, H., Otofuji, Y.I., 2009. Tectonic deformation of the Indochina Peninsula recorded in the Mesozoic palaeomagnetic results. Geophys. J. Int. 179 (1) https://doi.org/10.1111/j.1365-246X.2009.04274.x.
Tapponnier, P., Peltzer, G., Armijo, R., 1986. On the mechanics of the collision between India and Asia. Geological Society, London, Special Publications 19 (1), 113–157. https://doi.org/10.1144/GSL.SP.1986.019.01.07.
Taylor, M., Yin, A., 2009. Active structures of the Himalayan-Tibetan orogen and their relationships to earthquake distribution, contemporary strain field, and Cenozoic volcanism. Geosphere 5 (3). https://doi.org/10.1130/GES00217.1.
Thein, M., 2017. Current tectonic activity along the Sagaing Fault, Myanmar indicated by alluvial fans. Geolog. Soc. Memoir 48 (1). https://doi.org/10.1144/M48.20.
Thompson, J.O., Moulin, M., Aslanian, D., de Clarens, P., Guillocheau, F., 2019. New starting point for the Indian Ocean: second phase of breakup for Gondwana. Earth. Sci. Rev. 191 https://doi.org/10.1016/j.earscirev.2019.01.018.
Tilmann, F., Schurr, B., Yuan, X., Than, O., 2021. Myanmar subduction to collision imaging array (MySCOLAR). GFZ Data Services. Other/Seismic Network. https://doi.org/10.14470/1P7564636194.
Tiwari, A.K., Bhushan, K., Eken, T., Singh, A., 2018. Upper mantle dynamics of Bangladesh by splitting analysis of core-mantle refracted SKS, PKS, and SKKS phases. Phys Earth Planet Inter 279. https://doi.org/10.1016/j.pepi.2018.03.006.
Toyokuni, G., Zhao, D., Kurata, K., 2022. Whole-mantle tomography of southeast asia: new insight into plumes and slabs. https://doi.org/10.1002/essoar.10510681.1.
Vernant, P., Bilham, R., Szeliga, W., Drupka, D., Kalita, S., Bhattacharyya, A.K., Gaur, V. K., Pelgay, P., Cattin, R., Berthet, T., 2014. Clockwise rotation of the Brahmaputra Valley relative to India: tectonic convergence in the eastern Himalaya, Naga Hills, and Shillong Plateau. Solid Earth 119 (8). https://doi.org/10.1002/2014JB011196.
Vigny, C., 2003. Present-day crustal deformation around Sagaing fault, Myanmar. J. Geophys. Res. 108 (B11) https://doi.org/10.1029/2002jb001999.
Walker, K.T., Bokelmann, G.H.R., Klemperer, S.L., Nyblade, A., 2005. Shear wave splitting around hotspots: evidence for upwelling-related mantle flow?. In: Special paper of the geological society of America, 388. https://doi.org/10.1130/0-8137-2388-4.171.
Wang, M., Shen, Z.K., 2020. Present-Day crustal deformation of continental China derived from GPS and its tectonic implications. Solid Earth 125 (2). https://doi.org/10.1029/2019JB018774.
Wang, J., Zhao, D., 2008. P-wave anisotropic tomography beneath Northeast Japan. Phys. Earth Planet Interiors 170 (1–2). https://doi.org/10.1016/j.pepi.2008.07.042.
Wang, Y., Sieh, K., Tun, S.T., Lai, K.Y., Myint, T., 2014. Active tectonics and earthquake potential of the Myanmar region. Solid Earth 119 (4). https://doi.org/10.1002/2013JB010762.
Wang, X., Wei, S., Wang, Y., Maung Maung, P., Hubbard, J., Banerjee, P., Huang, B.S., Moe Oo, K., Bodin, T., Foster, A., Almeida, R., 2019. A 3-D Shear wave velocity model for Myanmar region. Solid Earth 124 (1). https://doi.org/10.1029/2018JB016622.
Wang, J., Su, Y., Zheng, J., Belousova, E.A., Chen, M., Dai, H., Zhou, L., 2020. Slab roll-back triggered back-arc extension south of the Paleo-Asian Ocean: insights from Devonian MORB-like diabase dykes from the Chinese Altai. Lithos. 376–377 https://doi.org/10.1016/j.lithos.2020.105790.
Wei, W., Xu, J., Zhao, D., Shi, Y., 2012. East Asia mantle tomography: new insight into plate subduction and intraplate volcanism. J. Asian Earth. Sci. 60 https://doi.org/10.1016/j.jseaes.2012.08.001.
Wessel, P., Luis, J.F., Uieda, L., Scharroo, R., Wobbe, F., Smith, W.H.F., Tian, D., 2019. The generic mapping tools version 6. Geochem., Geophys., Geosyst. 20 (11) https://doi.org/10.1029/2019GC008515.
Wu, S., Yao, J., Wei, S., Hubbard, J., Wang, Y., Min Htwe, Y.M., Thant, M., Wang, X., Wang, K., Liu, T., Liu, Q., Tong, P., 2021. New insights into the structural heterogeneity and geodynamics of the Indo-Burma subduction zone from ambient noise tomography. Earth Planet. Sci. Lett. 562 https://doi.org/10.1016/j.epsl.2021.116856.
Yan, Q., Shi, X., Metcalfe, I., Liu, S., Xu, T., Kornkanitnan, N., Sirichaiseth, T., Yuan, L., Zhang, Y., Zhang, H., 2018. Hainan mantle plume produced late Cenozoic basaltic rocks in Thailand, Southeast Asia. Sci. Rep. 8 (1) https://doi.org/10.1038/s41598-018-20712-7.
Yang, Z., Yin, J., Sun, Z., Otofuji, Y.ichiro, Sato, K., 2001. Discrepant Cretaceous paleomagnetic poles between Eastern China and Indochina: a consequence of the extrusion of Indochina. Tectonophysics. 334 (2) https://doi.org/10.1016/S0040-1951(01)00061-0.
Yang, T., Liu, F., Harmon, N., Le, K.P., Gu, S., Xue, M., 2014. Lithospheric structure beneath Indochina block from Rayleigh wave phase velocity tomography. Geophys. J. Int. 200 (3) https://doi.org/10.1093/gji/ggu488.
Yao, J., Liu, S., Wei, S., Hubbard, J., Huang, B.S., Chen, M., Tong, P., 2021. Slab models beneath central myanmar revealed by a joint inversion of regional and teleseismic traveltime data. Solid Earth 126 (2). https://doi.org/10.1029/2020JB020164.
Ye, Z., Li, Q., Gao, R., Zhang, H., Shen, X., Liu, X., Gong, C., 2016. Anisotropic regime across northeastern Tibet and its geodynamic implications. Tectonophysics. 671 https://doi.org/10.1016/j.tecto.2016.01.011.
Yu, Y., Gao, S.S., Liu, K.H., Yang, T., Xue, M., Le, K.P., Gao, J., 2018. Characteristics of the mantle flow system beneath the indochina peninsula revealed by teleseismic shear wave splitting analysis. Geochem., Geophys., Geosyst. 19 (5) https://doi.org/10.1029/2018GC007474.
Yu, Y., Chen, Y.J., Feng, Y., An, M., Liang, X., Guo, Z., Qu, W., Li, S., Dong, S., 2021. Asthenospheric flow channel from northeastern tibet imaged by seismic tomography between ordos block and Yangtze craton. Geophys. Res. Lett. 48 (17) https://doi.org/10.1029/2021GL093561.
Yu, X., Zhang, Y., Qian, X., Ghani, A.A., Sheldrick, T.C., Xu, C., Wang, Y., 2023. Southward continuation and slab rollback of the Neotethyan arc−back-arc system: insights from Eocene mafic intrusions from North Sumatra, SE Asia. GSA Bulletin. https://doi.org/10.1130/b36651.1.
Zahirovic, S., Seton, M., Müller, R.D., 2014. The Cretaceous and cenozoic tectonic evolution of Southeast Asia. Solid Earth 5 (1). https://doi.org/10.5194/se-5-227-2014.
Zhang, H., Liu, Y., Thurber, C., Roecker, S., 2007. Three-dimensional shear-wave splitting tomography in the Parkfield, California, region. Geophys. Res. Lett. 34 (24) https://doi.org/10.1029/2007GL031951.
Zhang, L.Y., Fan, W.M., Ding, L., Ducea, M.N., Pullen, A., Li, J.X., Sun, Y.L., Yue, Y.H., Cai, F.L., Wang, C., Peng, T.P., Sein, K., 2020. Quaternary volcanism in myanmar: a record of indian slab tearing in a transition zone from oceanic to continental subduction. Geochem., Geophys., Geosyst. 21 (8) https://doi.org/10.1029/2020GC009091.
Zhang, G., He, Y., Ai, Y., Jiang, M., Mon, C.T., Hou, G., Thant, M., Sein, K., 2021. Indian continental lithosphere and related volcanism beneath Myanmar: constraints from local earthquake tomography. Earth Planet. Sci. Lett. 567 https://doi.org/10.1016/j.epsl.2021.116987.
Zhao, D., Liu, L., 2010. Deep structure and origin of active volcanoes in China. Geosci. Front. 1 (1) https://doi.org/10.1016/j.gsf.2010.08.002.
Zhao, D., Toyokuni, G., Kurata, K., 2021. Deep mantle structure and origin of Cenozoic intraplate volcanoes in Indochina, Hainan and South China Sea. Geophys. J. Int. 225 (1) https://doi.org/10.1093/gji/ggaa605.
Zheng, T., He, Y., Ding, L., Jiang, M., Ai, Y., Mon, C.T., Hou, G., Sein, K., Thant, M., 2020. Direct structural evidence of Indian continental subduction beneath Myanmar. Nat. Commun. 11 (1) https://doi.org/10.1038/s41467-020-15746-3.